

**Preliminary Report
of
The Hakuho Maru Cruise KH-94-2
(Leg 1 & 2)**

May 17, 1994 – June 11, 1994

**Studies on reproduction and recruitment processes
of pelagic fish**

**Ocean Research Institute
University of Tokyo
2002**

**Preliminary Report
of
The Hakuho Maru Cruise KH-94-2
(Leg 1 & 2)**

May 17, 1994 – June 11, 1994

**Studies on reproduction and recruitment processes
of pelagic fish**

By

The Scientific Members of the Cruise

Edited by

Takashige SUGIMOTO

PREFACE

The main purpose of this cruise is to clarify spawning ecology and larval survival strategy of pelagic fish, particularly sardine, jack mackerel and anchovy. This cruise is the 4th time, followed by cruises around Tosa Bay in December 1988, around Satsunan off Shikou in February-March 1991 and around Tosa Bay-off Bousou in February-March 1994.

In first part of 1990s, sardine stock rapidly decreased. Anchovy and saury was taking over sardine. This period is corresponding to a period that jack mackerel stock does not show strong recovery. As mechanism of these dominant changes of species, sardine abundance leading hypothesis, three-species interaction hypothesis and zooplankton grazing trigger hypothesis are arisen. However, statistical data verifying these hypotheses is not provided and this issue is one of scope for GLOBEC (Global Ocean Ecosystem Dynamics) studies.

First and second legs were focused on the Ensu-nada Sea and off shore region of Izu, and offshore region of Izu and the Kuroshio Extension – the Kuroshio-Oyashio transition regions, respectively. The former leg was focused, firstly, on movement of the Kuroshio water into coastal regions, larval transport associated with the movement, and structure and its fluctuation of survival environment for the fish larvae (ex. Distributions of chlorophyll and copepod), and secondly on spawning behavior and physiological ecology of adult jack mackerel in the northern part of the Izu Islands. The latter leg was focused on distribution of zooplankton, phytoplankton and fish larvae, vertical migration, larval transport and feeding environment in fronts of the Kuroshio Extension, warm streamers and warm core rings.

We had some accidents such as nets breaking associated with large blooming of diatom in the first leg and with high concentration of small Thaliacea in the second leg. An Argos buoy deployed in the warm streamer located in the front was entrained into the warm core ring off Kinkazan after northward movement. Current velocity and particle transporting function of the warm streamer detected by floating buoys and ADCP were considerably larger than our previous estimates.

Fortunately, since we had very good weather condition and enthusiastic cooperation by ship crews, 100% of scheduled observation had been conducted. We would like to express our deep appreciation to the crews.

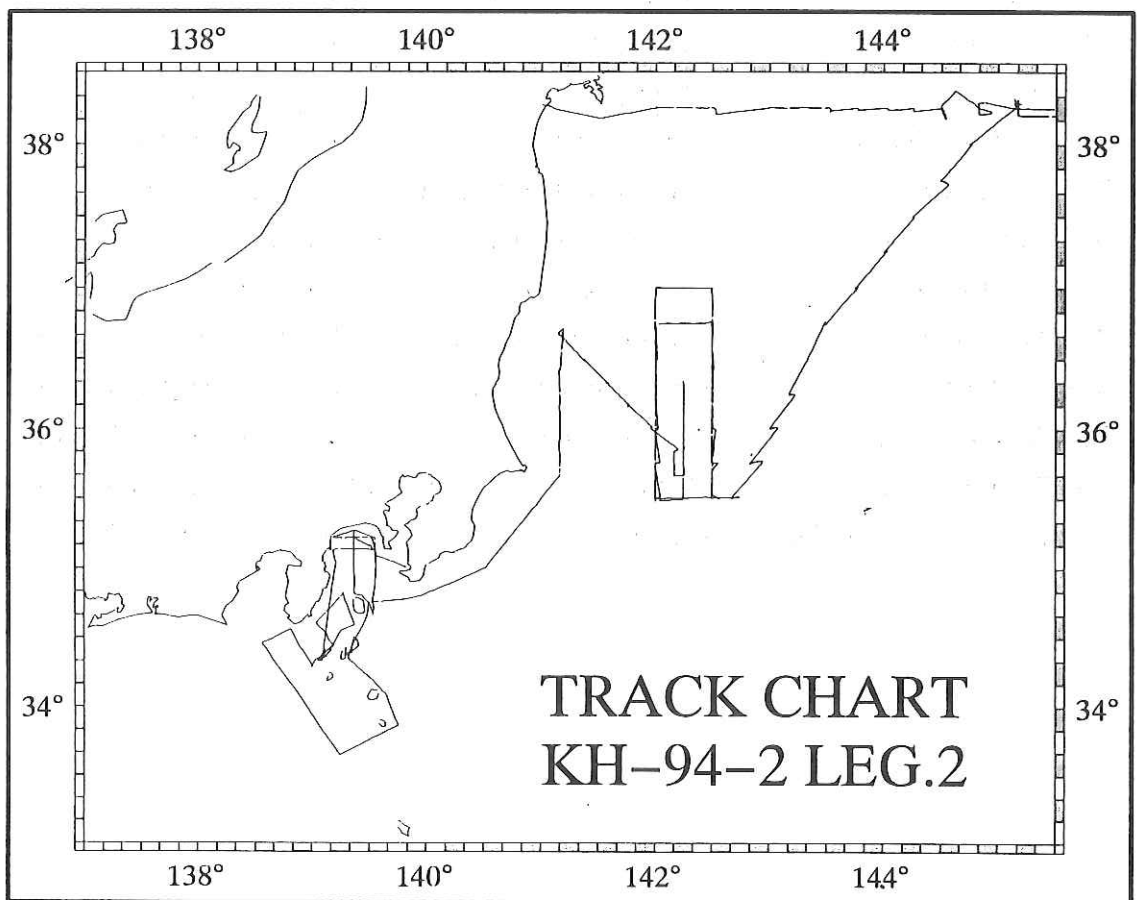
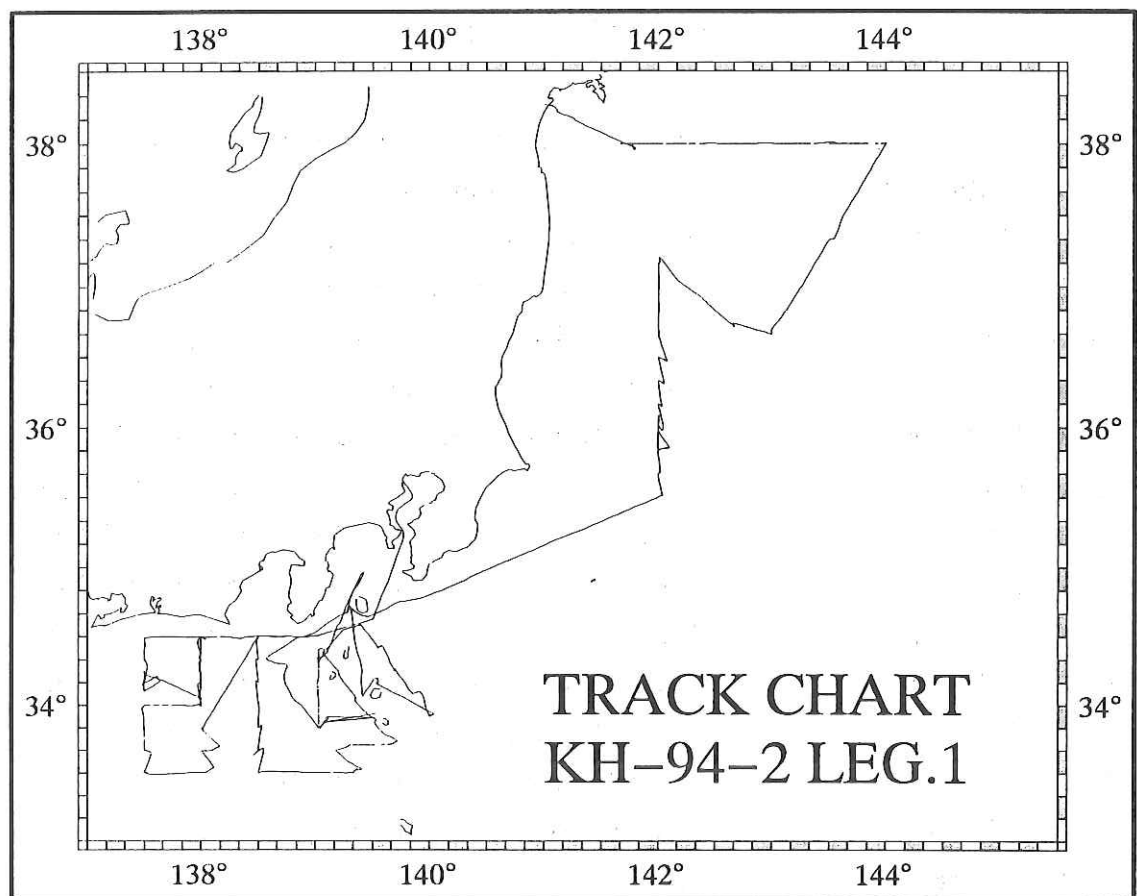
Takashige Sugimoto
Chief Scientist

Contents

List of Scientists aboard.....	1
Track Charts.....	2
Time Table.....	3
Scientific Papers and Summarized Results.....	8
CTD Data.....	43

Scientists aboard

SUGIMOTO Takashige	Ocean Research Institute, the University of Tokyo
OTSUKA Kazuyuki	Tokyo University of Fisheries
YAMAZAKI Hidekatsu	Tokyo University of Fisheries
ENDO Yoshishige	Faculty of Agriculture, Tohoku University
KASAI Akihide	Faculty of Agriculture, Kyoto University
AOKI Ichiro	Ocean Research Institute, the University of Tokyo
NAKATA Hideaki	Ocean Research Institute, the University of Tokyo
KOMATSU Teruhisa	Ocean Research Institute, the University of Tokyo
KIMURA Shingo	Ocean Research Institute, the University of Tokyo
KISHI Michio	Ocean Research Institute, the University of Tokyo
INAGAKI Tadashi	Ocean Research Institute, the University of Tokyo
KOIZUMI Kin-ichiro	Ocean Research Institute, the University of Tokyo
IGARASHI Chiaki	Ocean Research Institute, the University of Tokyo
NAGAE Hideo	Ocean Research Institute, the University of Tokyo
OKAZAKI Yuji	Faculty of Agriculture, Miyazaki University
OBARA Masahiro	Tokyo University of Fisheries
MATSUBARA Kosuke	Tokyo University of Fisheries
OTA Takashi	Faculty of Agriculture, Tohoku University
SATO Keisuke	Faculty of Agriculture, Tohoku University
OSHIMA Tatsuki	Faculty of Agriculture, Tohoku University
NAKAKURA Chihaya	Faculty of Agriculture, the University of Tokyo
IIDA Tomohiro	Faculty of Agriculture, the University of Tokyo
NEGAMI Ken	Faculty of Agriculture, the University of Tokyo
MIYASHITA Kazushi	Ocean Research Institute, the University of Tokyo
YAMADA Tomohide	Ocean Research Institute, the University of Tokyo
Kawser AHMED	Ocean Research Institute, the University of Tokyo
FURUSHIMA Yasuo	Ocean Research Institute, the University of Tokyo
TATOKORO Kazuaki	Ocean Research Institute, the University of Tokyo
Susana SAINZ-TRAPAGA	Ocean Research Institute, the University of Tokyo



KH94-2 LEG-1 (Position Log) No.2

St. No.	Lat.	Long.	Day	Time	Dep. (m)	CTD	XBT	Ros.	W.S.(0)	Chl.(0)	ORI-S	ORI-O	ORI-H	Norp.	MTD	IKPT	Ch.t.
X9415	34.20.12N	139.01.94E	21.May.94	17:10	122												
X9416	34.08.83N	139.01.93E	21.May.94	17:20	343												
X9417	34.07.02N	139.01.95E	21.May.94	17:30	705												
X9418	34.05.23N	139.01.95E	21.May.94	17:40	567												
X9419	34.03.50N	139.01.91E	21.May.94	17:50	391												
X9420	34.01.80N	139.01.80E	21.May.94	18:00	118												
X9421	34.00.14N	139.01.38E	21.May.94	18:10	58												
X9422	34.00.45N	139.01.37E	21.May.94	18:20	164												
X9423	34.00.64N	139.01.47E	21.May.94	18:30	520												
X9424	34.00.86N	139.01.58E	21.May.94	18:40	554												
X9425	34.03.10N	139.01.74E	21.May.94	18:50	652												
X9426	34.01.50N	139.01.99E	21.May.94	19:00	830												
X9427	33.09.91N	139.02.05E	21.May.94	19:10	1909												
X9428	33.08.22N	139.02.09E	21.May.94	19:20	2373												
X9429	33.06.58N	139.02.09E	21.May.94	19:30	3007												
X9430	33.04.91N	139.02.05E	21.May.94	19:40	3007												
X9431	33.03.26N	139.02.02E	21.May.94	19:50	3007												
X9432	33.01.51N	139.02.07E	21.May.94	20:00	3007												
K-25	33.50.11N	139.02.18E	21.May.94	20:51	1336												
X9433	33.51.65N	139.00.07E	21.May.94	23:40	1358												
X9434	33.53.03N	138.59.26E	21.May.94	23:50	2055												
X9435	33.54.42N	138.57.95E	24.May.94	0:00	3007												
X9436	33.55.83N	138.56.62E	24.May.94	0:10	3007												
X9437	33.57.30N	138.55.27E	24.May.94	0:20	3007												
X9438	33.58.80N	138.53.88E	24.May.94	0:30	3007												
K-24	34.00.18N	138.52.47E	22.May.94	0:49	112												
X9439	34.03.74N	138.47.77E	22.May.94	2:20	280												
X9440	34.05.38N	138.46.92E	22.May.94	2:28	550												
X9441	34.06.48N	138.46.20E	22.May.94	2:35	1057												
X9442	34.08.04N	138.45.19E	22.May.94	2:45	1487												
X9443	34.09.62N	138.44.26E	22.May.94	2:55	1683												
K-23	34.10.48N	138.43.98E	22.May.94	3:08	1791												
K-22	34.20.06N	138.34.70E	22.May.94	6:24	1607												
K-28	34.30.26N	138.55.19E	22.May.94	9:20	644												
K-34	34.39.90N	139.15.02E	22.May.94	11:20	444												
S-1	34.24.95N	139.06.41E	23.May.94	0:00	670												
K-35	34.35.03N	139.23.57E	23.May.94	2:50	226												
K-36	34.24.94N	139.33.05E	23.May.94	4:40	642												
K-37	34.15.05N	139.41.89E	23.May.94	6:40	879												
K-38	34.05.13N	139.51.84E	23.May.94	9:00	1111												
K-39	33.55.26N	140.00.47E	23.May.94	11:07	1042												
K-40	35.30.02N	142.00.11E	24.May.94	8:30	4607												

KH94-2 LEG-1 (Position Log) №0.3

St. №.	Lat.	Long.	Day	Time	Dep. (m)	XBT	Ros.	W.S.(0)	Chl.(0)	ORI-S	ORI-O	ORI-H	Norp.	MTD	IKPT	Ch. t.
K-41	35°40.18'N	142°00.35'E	24.May.94	10:39	3719	○				○						
K-42	35°50.00'N	142°00.15'E	24.May.94	12:20	3247	○				○						
K-43	36°00.23'N	142°00.09'E	24.May.94	18:24	3343	○				○						
K-44	36°10.01'N	142°00.08'E	24.May.94	20:38	6016	○				○						
K-45	36°19.93'N	142°00.26'E	24.May.94	22:55	6017	○				○						
K-46	36°30.00'N	142°00.10'E	25.May.94	1:05	6686	○				○						
K-47	36°40.02'N	142°00.02'E	25.May.94	3:25	2512	○				○						
K-48	36°49.09'N	142°00.14'E	25.May.94	5:18	2505	○				○						
K-49	36°59.90'N	142°00.14'E	25.May.94	7:14	1356	○				○						
K-50	37°09.97'N	142°00.14'E	25.May.94	9:37	1021	○				○						
K-52	37°02.94'N	142°10.07'E	25.May.94	11:56	1916	○				○						
K-53	36°57.15'N	142°19.97'E	25.May.94	12:44	2556	○				○						
K-54	36°50.02'N	142°30.00'E	25.May.94	14:09	3794	○				○						
K-55	36°43.38'N	142°39.99'E	25.May.94	14:59	5400	○				○						
K-56	36°32.00'N	142°50.35'E	25.May.94	16:14	5591	○				○						
K-57	36°39.90'N	143°00.14'E	25.May.94	17:00	5940	○				○						
K-58	36°50.00'N	143°07.60'E	25.May.94	18:14	6419	○				○						
K-59	36°59.91'N	143°15.18'E	25.May.94	19:00	6744	○				○						
K-60	37°10.00'N	143°22.65'E	25.May.94	20:09	7040	○				○						
K-61	37°20.00'N	143°30.51'E	25.May.94	20:55	7038	○				○						
K-62	37°30.12'N	143°37.61'E	25.May.94	22:09	6650	○				○						
K-63	37°39.91'N	143°45.35'E	25.May.94	22:55	7205	○				○						
K-64	37°50.13'N	143°52.55'E	26.May.94	0:13	6945	○				○						
K-65	38°00.00'N	144°00.10'E	26.May.94	1:03	7443	○				○						
K-66	38°00.03'N	143°45.00'E	26.May.94	3:20	5858	○				○						
K-67	38°00.19'N	143°33.41'E	26.May.94	4:26	4543	○				○						
K-68	37°59.96'N	143°15.09'E	26.May.94	5:49	2870	○				○						
K-69	37°59.90'N	143°00.03'E	26.May.94	6:35	1867	○				○						
K-70	38°00.00'N	142°45.00'E	26.May.94	8:11	1484	○				○						
K-71	38°00.03'N	142°30.32'E	26.May.94	9:00	1125	○				○						
K-72	37°59.96'N	142°14.46'E	26.May.94	10:19	720	○				○						
K-73	37°59.98'N	141°59.85'E	26.May.94	11:02	363	○				○						
K-74	37°59.05'N	144°46.20'E	26.May.94	12:30	220	○				○						O

KH94-2 LEG-2 (Position Log) №0.2

St. №.	Lat.	Long.	Day	Time	Dep. (m)	CTD	XBT	Ros.	W.S(0)	Chl.(0)	ORI-S	ORI-O	ORI-H	Norp.	MTD	IKPT	Chl. t.
K-110	35°45.24N	142°31.72E	5.Jun.94	13:18	5808	○											
K-111	35°30.19N	142°30.44E	5.Jun.94	15:22	6855	○											
E-3	35°45.00N	142°30.04E	5.Jun.94	17:27	5728												
E-4	36°00.00N	142°29.98E	5.Jun.94	18:21	5629												
E-5	36°14.95N	142°29.98E	5.Jun.94	19:17	9795												
E-6	36°29.95N	142°30.01E	5.Jun.94	20:12	5661												
E-7	36°45.17N	142°30.07E	5.Jun.94	21:08	7029												
E-10	36°44.99N	141°59.97E	5.Jun.94	22:35	2524												
E-11	36°29.77N	142°00.02E	5.Jun.94	23:30	2775												
E-12	36°14.88N	142°00.05E	6.Jun.94	0:22	2900												
E-13	36°59.94N	141°59.98E	6.Jun.94	1:14	2407	○											
E-14	35°45.03N	142°00.14E	6.Jun.94	2:11	4124												
E-15	35°30.00N	142°00.05E	6.Jun.94	3:11	4621												
E-16	35°30.07N	142°15.03E	6.Jun.94	3:54	7235												
E-17	35°45.80N	142°15.02E	6.Jun.94	4:48	4668												
E-18	35°59.92N	142°14.90E	6.Jun.94	5:40	4299												
E-19	36°14.97N	142°14.96E	6.Jun.94	6:35	3893												
K-112	35°50.30N	142°10.29E	6.Jun.94	10:33	3972	○	○	○									
K-113	35°59.81N	141°57.72E	6.Jun.94	13:05	2997	○	○	○									
K-114	36°09.79N	141°55.89E	6.Jun.94	15:20	1969	○											
K-115	36°19.89N	141°54.07E	6.Jun.94	18:05	171	○											
K-116	36°29.93N	141°22.08E	6.Jun.94	20:44	987	○											
K-117	36°39.90N	141°09.89E	6.Jun.94	23:26	261	○											
K-118	36°24.97N	141°09.88E	7.Jun.94	3:25	757	○											
K-119	36°09.90N	141°09.91E	7.Jun.94	4:51	717	○											
K-120	35°55.02N	141°09.84E	7.Jun.94	6:30	477	○											

Biological productivity of meso-scale eddies caused by frontal disturbances in the Kuroshio

Shingo Kimura, Akihide Kasai, Hideaki Nakata,
Takashige Sugimoto, John H. Simpson, and
Joseph V. S. Cheok



Kimura, S., Kasai, A., Nakata, H., Sugimoto, T., Simpson, J. H., and Cheok, J. V. S. 1997. Biological productivity of meso-scale eddies caused by frontal disturbances in the Kuroshio. – ICES Journal of Marine Science, 54: 179–192.

Temporal and spatial changes in nutrient and chlorophyll distributions caused by frontal disturbances of the Kuroshio, a western boundary current in the Pacific Ocean, are presented. The regions of high nitrate and phosphate concentrations are associated with an eddy of positive vorticity which separates from the Kuroshio front within a few days of generation. The nutrients supplied to the euphotic layer by upwelling and mixing in the cyclonic eddy accelerate primary production in the frontal region. The specific growth rate calculated from temporal changes in chlorophyll and nitrate concentrations, of 0.8 d^{-1} is considerably larger in the offshore region. According to a numerical simulation made using a turbulent closure model a chlorophyll maximum occurs during the fifth day after the generation of the eddy and the growth rate in the euphotic layer is in good agreement with that estimated from observations. After the peak production the growth becomes nutrient limited. Since the frontal disturbances occur in association with short-term fluctuations in the Kuroshio frontal meander, which has a period of a few weeks, the biological production enhancement by this kind of eddy is expected to occur with similar frequency. It is estimated that the total annual nitrogen input to the region via the eddies could result in a carbon production rate of $40 \text{ gC m}^{-2} \text{ y}^{-1}$.

© 1997 International Council for the Exploration of the Sea

Key words: Kuroshio, eddy, frontal disturbance, primary production, physical-biological model.

Received 12 January 1996; accepted 11 December 1996.

S. Kimura, H. Nakata and T. Sugimoto: Ocean Research Institute, University of Tokyo, 1-15-1, Minamidai, Nakano-ku, Tokyo, 164, Japan. A. Kasai: Faculty of Agriculture, Kyoto University, Kyoto, 606-01, Japan. J. H. Simpson and J. V. S. Cheok: School of Ocean Sciences, University of Wales, Bangor, Menai Bridge, Gwynedd, LL59 5EY, UK.

Introduction

Cyclonic circulations in frontal eddies associated with the wave-like meander of the western boundary current have been well described from satellite imagery and hydrographic observations, particularly in the Gulf Stream front between the Florida Straits and Cape Hatteras. In this region, meanders of several hundred kilometres wavelength and amplitudes of a few tens of kilometres propagate to the north-west. The southward movements of the tongue-like extrusions of the Gulf Stream derived from the wave crest generate a cold upwelled core in the wave trough about every two weeks (Lee *et al.*, 1981). The phase velocity of the wave is estimated to be $40\text{--}50 \text{ cm s}^{-1}$ (Legeckis, 1979; Lee *et al.*, 1981), although the horizontal scales are

dependent on bottom topography (Legeckis, 1979; Bane and Brooks, 1979). The eddies travel northward with the same phase velocity as the wave and contribute to a rapid shelf-Gulf Stream water exchange. Cross-stream horizontal scales of the eddy are in the order of a few tens of kilometres and the along-stream scales are larger than the cross-stream scales. In the cyclonic eddy, nutrients are supplied to the euphotic layer by upwelling and accelerate primary production in the frontal region (Lee *et al.*, 1981; Yoder *et al.*, 1981). Since eddies are frequently generated there is considerable enhancement of biological productivity in the coastal water. According to a calculation by Lee *et al.* (1981), the annual carbon production by phytoplankton in the Gulf Stream front is in the range $32\text{--}64 \text{ gC m}^{-2} \text{ y}^{-1}$.

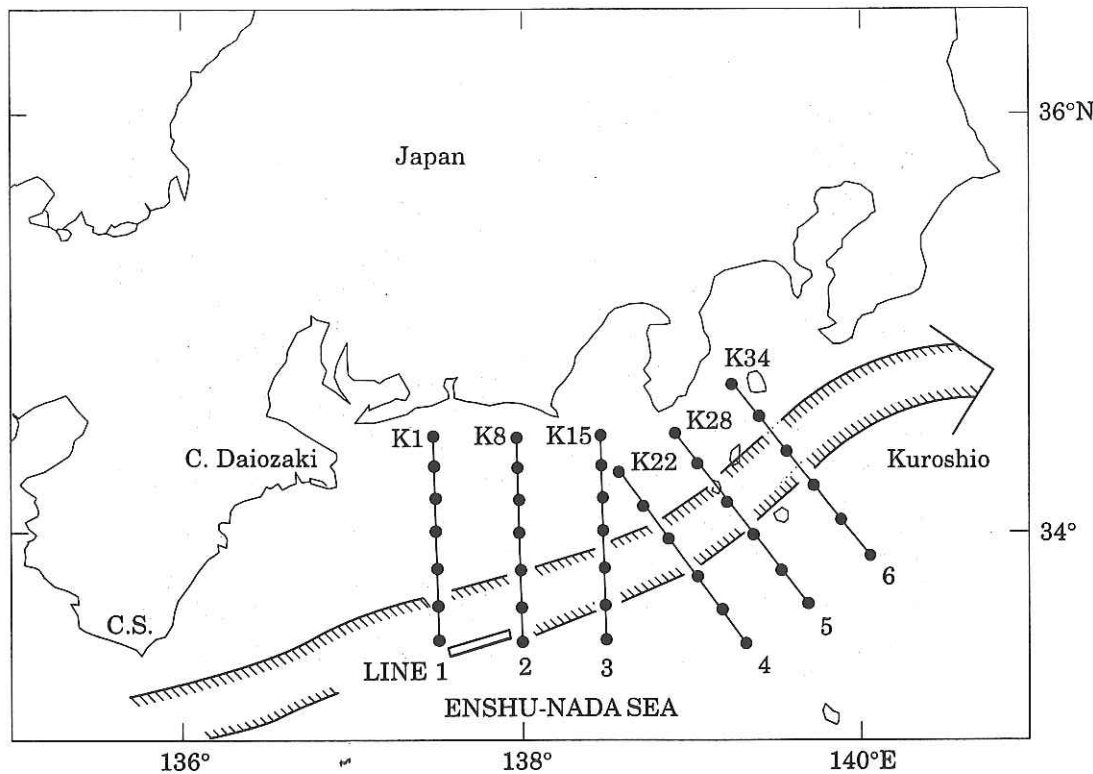


Figure 1. Observational locations. Solid circles indicate the stations (K1–39).

Similar frontal disturbances are also recognized in the Kuroshio region off the Japanese coast, a well known counterpart of the Gulf Stream in the Pacific Ocean. In the Kuroshio region, wave-like meanders with wavelengths of 100, 200, 400 km occur with periods of 5–8, 10–12 and 17–19 days respectively, west of Cape Shionomisaki in the Enshu-nada Sea (Kimura and Sugimoto, 1993) and generate frontal cyclonic eddies. Given the results in the Gulf Stream, it would seem likely that these eddies will enhance the biological productivity in the sea. In fact the coastal regions are well known as nursery grounds of the Japanese sardine and anchovy larvae. However, no adequate explanation of the high biological productivity has previously been given despite many studies on coastal upwelling by wind and topography. In this paper we describe the vertical and horizontal structure of a cyclonic eddy caused by frontal disturbances in the Kuroshio and its contribution to primary production in the coastal area.

Observations

Hydrographic observations with a conductivity-temperature-depth profiler (CTD) and water sampling were carried out at 39 stations in the Enshu-nada Sea along six sections during 18–23 May, 1994, as shown in Figure 1. The CTD locations were determined after detection of a target eddy using satellite imagery. It was important that the CTD lines passed through the centre of the eddy for analysis of primary production. An

AVHRR satellite image on 17 May 1994 (Fig. 2) shows the target eddy in a frontal disturbance of the north wall of the Kuroshio off Cape Daiozaki at 137°E. The eddy is characterized by an 80 km diameter, cyclonic cold region accompanied by westward movement of a tongue-like streamer.

During the observational period the Kuroshio took a “non-large” meander path, termed “N-type” by Japanese scientists, located close to the Japanese coast with small scale meandering. The eddy is situated in the trough of the meander with 150 km horizontal wavelength. According to successive satellite images the crest and trough of the meander moved downstream with a phase velocity of 60 cm s^{-1} , which is almost the same as the current speed around the eddy measured using a ship-mounted, acoustic Doppler current profiler (ADCP). Apparently, the eddy moves downstream with the wave trough and the properties of the water mass in the trough conserved. The observational lines were designed to be located in the centre of the trough assuming the eddy was moving at 60 cm s^{-1} along the trough. During the observational period, the eddy, shown in Figure 2, lies on Line 1 on 18 May and on Line 3 on 20 May. However, since the observations on Line 2 were done on two separate days because of other observations in the region, the line was not located in the centre of the eddy.

Water samples were taken at selected depths with Niskin bottles mounted on a rosette sampler coupled to the CTD. Concentrations of phosphate, nitrate and

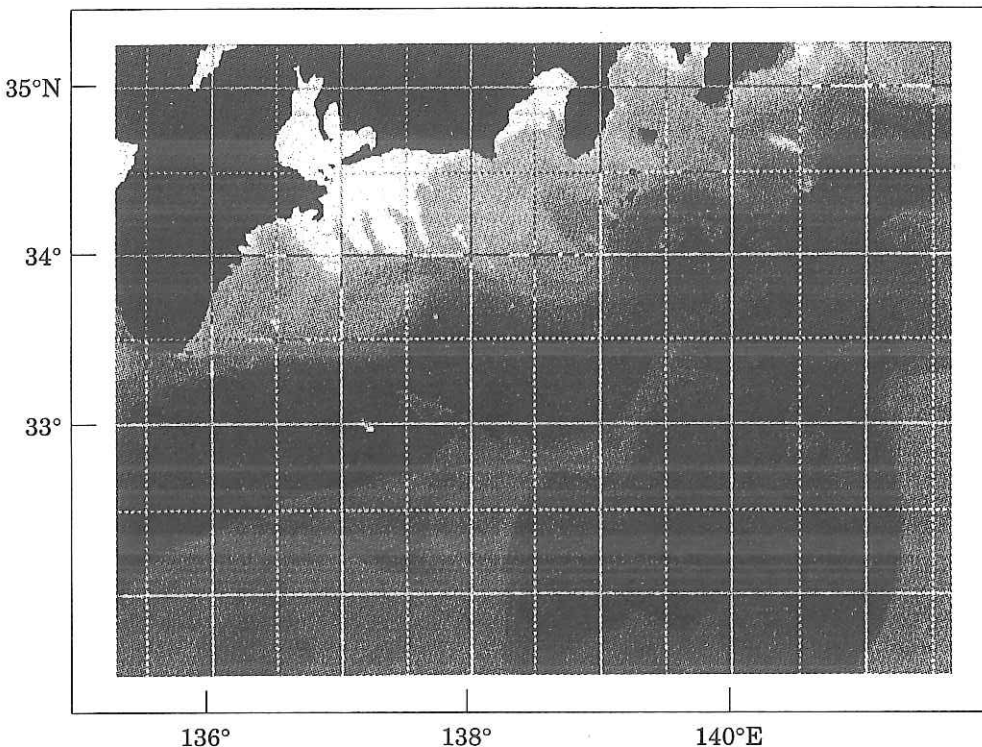


Figure 2. Satellite image of the Kuroshio on 17 May, 1994.

chlorophyll were obtained at depths of 0, 30, 50, 100, 200, 300, 500 and 1000 m on Line 2, and 0 m on other lines.

Numerical model

In order to obtain a description of the vertical structure of the eddy, we have utilized a one-dimensional model of vertical structure which includes turbulence closure. In the model, we simulated physical and biological variation in the isolated eddy which has detached from the Kuroshio frontal system, assuming a constant horizontal eddy diffusivity estimated from the observations. The model aims to provide, in particular, a value of the chlorophyll concentration when the nutrients are exhausted and changes of time-dependent growth rates of phytoplankton. These values are compared with those estimated from the observations. All the physical and biological symbols used in the equations are defined in Table 1.

Physical structure

The water column between the centre and the edge of the eddy is subject to the equations of motion in the x and y directions (x positive from the centre toward the edge of the eddy, y positive along flow direction in the eddy) depending on time t, depth z (increasing positively from the bottom layer of the eddy) and horizontal pressure gradients:

$$\frac{\partial u}{\partial t} = -\frac{1}{\rho} \frac{\partial P}{\partial x} + fv + \frac{\partial}{\partial z} \left(N_z \frac{\partial u}{\partial z} \right) \quad (1)$$

$$\frac{\partial v}{\partial t} = -fu + \frac{\partial}{\partial z} \left(N_z \frac{\partial v}{\partial z} \right) \quad (2)$$

$$\frac{1}{\rho} \frac{\partial P}{\partial x} = \frac{g}{\rho} (h - z) \frac{\partial \rho}{\partial x} + g \frac{\partial \bar{\eta}}{\partial x} \quad (3)$$

where u and v are current velocities in the x and y directions and f is the Coriolis parameter. In this case the horizontal pressure gradient in the y direction and the centrifugal force are neglected. For estimations of horizontal gradients (x direction) of physical and biological factors, the radius of the eddy is assumed to be 40 km. The horizontal pressure gradient term in Equation (1) is given by Equation (3) which is composed of a horizontal density gradient and a mean slope.

Horizontal advection and vertical diffusion of salinity and temperature at each level are given by

$$\begin{aligned} \frac{\partial (S, T)}{\partial t} = & -u \frac{\partial (S, T)}{\partial x} + \frac{\partial}{\partial z} \left(K_z \frac{\partial (S, T)}{\partial z} \right) \\ & + \frac{\partial}{\partial x} \left(K_h \frac{\partial (S, T)}{\partial x} \right) \end{aligned} \quad (4)$$

N_z in Equations (1) and (2), and K_z in Equation (4) are coefficients of vertical eddy viscosity and vertical eddy diffusivity respectively. K_h in Equation (4) is an

Table 1. Definitions, values and units of symbols used in the model.

Symbol	Definition	Value	Units
Physical variables and parameters			
u	current velocity in x-direction	—	m s^{-1}
v	current velocity in y-direction	—	m s^{-1}
P	pressure	—	—
ρ	density	—	kg m^{-3}
η	vertical displacement of water surface	—	m
f	Coriolis parameter	—	s^{-1}
S	salinity	—	no units
T	temperature	—	$^{\circ}\text{C}$
E	kinematic energy	—	$\text{m}^2 \text{s}^2$
q	turbulent intensity	—	m s^{-1}
N_z	coefficient of vertical eddy viscosity	—	$\text{m}^2 \text{s}^{-1}$
K_z	coefficient of vertical eddy diffusivity	—	$\text{m}^2 \text{s}^{-1}$
K_h	coefficient of horizontal eddy diffusivity	2.0E4	$\text{m}^2 \text{s}^{-1}$
ws	wind speed	5	m s^{-1}
Biological variables and parameters			
C	concentration of chlorophyll	—	$\mu\text{g l}^{-1}$
F	concentration of nitrogen in plankton	—	μM
D	concentration of dissolved inorganic nitrogen	—	μM
μ	phytoplankton specific growth rate	—	day^{-1}
γ	phytoplankton nitrogen uptake rate	—	$\mu\text{MN}(\mu\text{g l}^{-1} \text{chl})^{-1} \text{day}^{-1}$
κ	grazing rate by zooplankton	0.54	day^{-1}
ε	excreted proportion of grazed nutrient	0.50	—
γ_m	maximum DIN uptake rate	2.0	$\mu\text{M N day}^{-1}$
D_h	half saturation constant for DIN uptake	0.3	μM
μ_{light}	light related growth rate	—	day^{-1}
μ_{nitrogen}	nitrogen related growth rate	—	day^{-1}
I	layer mean irradiance	—	Wm^{-2}
μ'	maximum growth rate	1.2	day^{-1}
α	gross photosynthesis per unit irradiance at low illumination	4.1	$\mu\text{gC}(\mu\text{g chl})^{-1} \text{day}^{-1}(\text{Wm}^{-2})^{-1}$
β	biomass related respiration rate	3.0	$\mu\text{gC}(\mu\text{g chl})^{-1} \text{day}^{-1}$
R	chlorophyll:carbon ratio	0.033	$\mu\text{g chl} (\mu\text{gC})^{-1}$
Q	phytoplankton nitrogen quota	—	$\mu\text{MN}(\mu\text{g l}^{-1} \text{chl})^{-1}$
k_Q	minimum nitrogen quota	0.2	$\mu\text{MN}(\mu\text{g l}^{-1} \text{chl})^{-1}$
I_0	daily-averaged surface irradiance	80.0	Wm^{-2}
D_{input}	DIN input from bottom	—	$\mu\text{M} (\text{m}^{-2} \text{s}^{-1})^{-1}$
$K_{z_{\text{bottom}}}$	diffusivity in bottom boundary layer	—	$\text{m}^2 \text{s}^{-1}$
D_{flux}	difference of concentration of DIN at bottom	—	μM
Observational data			
$1/\rho \partial\rho/\partial x$	horizontal gradient of density	- 3.0E-8	m^{-1}
$\partial S/\partial x$	horizontal gradient of salinity	2.5E-6	m^{-1}
$\partial T/\partial x$	horizontal gradient of temperature	5.0E-5	$^{\circ}\text{C m}^{-1}$
$\partial C/\partial x$	horizontal gradient of chlorophyll con.	0.0	$\mu\text{g l}^{-1} \text{m}^{-1}$
$\partial F/\partial x$	horizontal gradient of nit. in plan. con.	0.0	$\mu\text{M m}^{-1}$
$\partial D/\partial x$	horizontal gradient of DIN con.	- 1.0E-4	$\mu\text{M m}^{-1}$
Differential scale			
Δt	simulation time step	0.002	day^{-1}
Δz	simulation depth increment	5.0	m

horizontal eddy diffusivity. This value is estimated to be $2 \times 10^3 \text{ m}^2 \text{s}^{-1}$ from the eddy evolution of area on Lines 1 and 3. A level 2.2 turbulence closure scheme is used to calculate vertical profiles of N_z and K_z as functions of local stability (Mellor and Yamada, 1982; Simpson et al., 1996) via

$$N_z = S_M l q; K_z = S_H l q$$

where S_M and S_H are stability functions depending on the local gradient Richardson number, q is the turbulent intensity and l is the turbulent length-scale given by

$$l = kz(1 - z/h)^{1/2} \quad (6)$$

where z is the height above the bottom of the eddy, h is the water depth and k is von Karman's constant. The

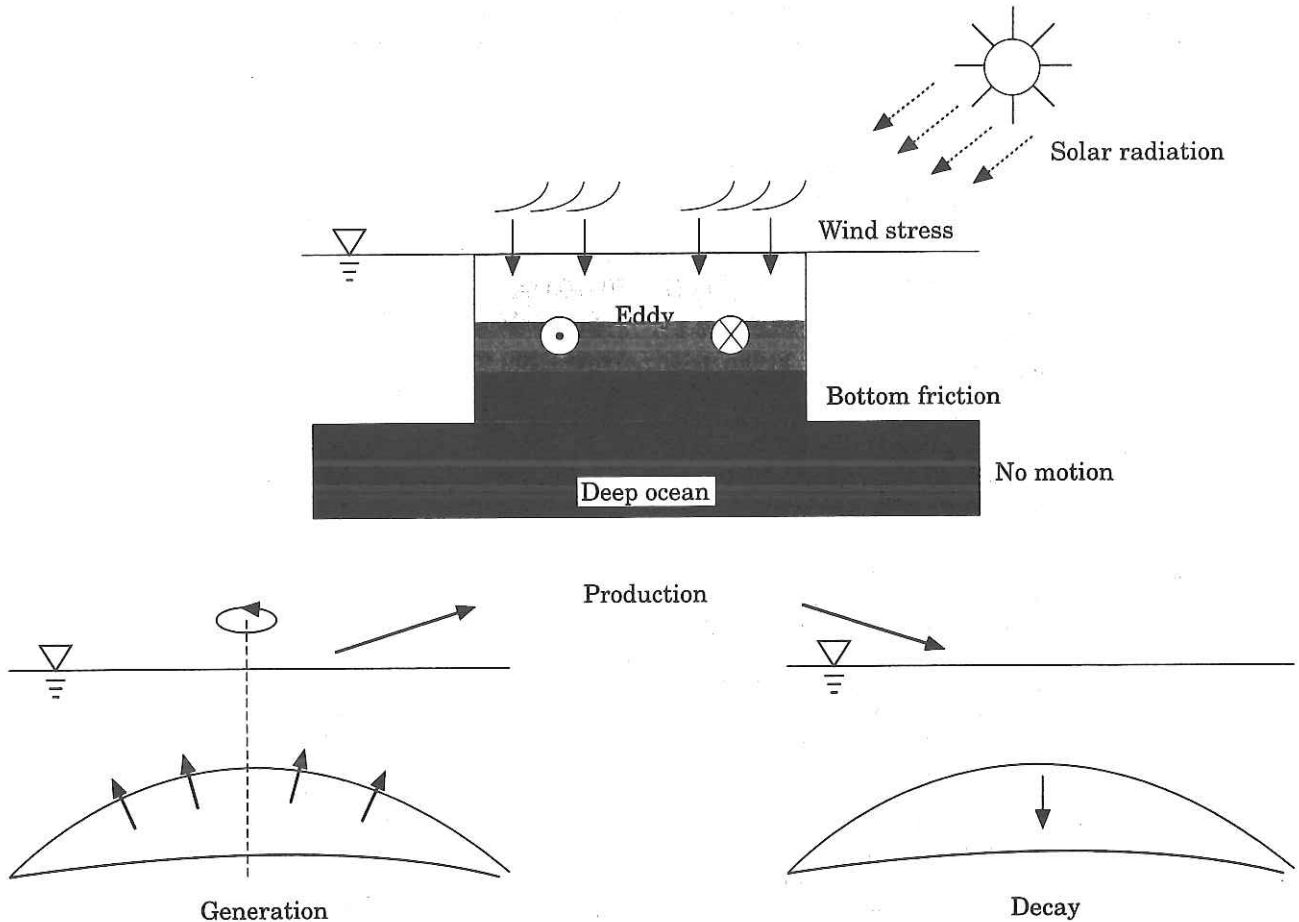


Figure 3. Schematic view of the eddy. Darker shade at the production stage indicates high concentration of nutrients and cold temperature. The generation and decay stages show movements of the eddy bottom.

turbulent intensity is calculated in the turbulent energy equation as follows:

$$\frac{\partial E}{\partial t} = \frac{\partial}{\partial z} \left(N_z \frac{\partial E}{\partial z} \right) + N_z \left[\left(\frac{\partial u}{\partial z} \right)^2 + \left(\frac{\partial v}{\partial z} \right)^2 \right] + K_z \left(\frac{g}{\rho} \frac{\partial p}{\partial z} \right) - \frac{q^3}{B_1 l} \quad (7)$$

where E is the turbulent kinetic energy (TKE) calculated by $E = q^2/2$. The first term on the right of Equation (7) is vertical diffusion of turbulent kinetic energy. The second and third terms are shear and buoyancy production of TKE. The fourth term is dissipation.

As boundary conditions, we use a quadratic stress law for both the bottom stress at the bottom of the eddy and wind stress at the sea surface. The wind velocity is taken as 5 m s^{-1} , which was the mean observed by the research vessel during the observational period. Surface heating is controlled by the formulation of Edinger *et al.* (1968) described in Simpson and Bowers (1984). After generation, the eddy disappeared in a week. In this model all horizontal gradients given in the initial condition decrease linearly with time and an initial velocity in the y direction is assumed to be 30 cm s^{-1} . Figure 3 shows a schematic view of the developed eddy. The eddy

causes an uplift of cooled nutrient-rich water to the euphotic layer at the generation stage. Vertical mixing supplies nutrients for growth of phytoplankton to the surface layer (production stage). The supply is gradually terminated associated with eddy spin down (decay stage). Physical structures at the generation and decay stages are not reproduced in this model.

Biological structure

The biological scheme is described by three non-linearly coupled differential equations:

$$\frac{\partial C}{\partial t} = -u \frac{\partial C}{\partial x} + \frac{\partial}{\partial z} \left(K_z \frac{\partial C}{\partial z} \right) + \frac{\partial}{\partial x} \left(K_h \frac{\partial C}{\partial x} \right) + \mu C - \kappa C \quad (8)$$

$$\frac{\partial F}{\partial t} = -u \frac{\partial F}{\partial x} + \frac{\partial}{\partial z} \left(K_z \frac{\partial F}{\partial z} \right) + \frac{\partial}{\partial x} \left(K_h \frac{\partial F}{\partial x} \right) + \gamma C - \kappa F \quad (9)$$

$$\frac{\partial D}{\partial t} = -u \frac{\partial D}{\partial x} + \frac{\partial}{\partial z} \left(K_z \frac{\partial D}{\partial z} \right) + \frac{\partial}{\partial x} \left(K_h \frac{\partial D}{\partial x} \right) + \gamma C - \varepsilon \kappa F \quad (10)$$

where C is the concentration of phytoplankton chlorophyll, F , the concentration of the phytoplankton nitrogen and D , the dissolved inorganic nitrogen in the eddy.

Vertical turbulent diffusivity, K_z , is the same value estimated in the physical model.

The phytoplankton growth rate, μ , is determined by light and nutrient-controlled phytoplankton growth as follows (Tett *et al.*, 1986).

$$\mu = \min(\mu_{\text{light}}, \mu_{\text{nitrogen}}) \quad (11)$$

$$\mu_{\text{light}} = (\alpha_1 - \beta)R \quad (12)$$

$$\mu_{\text{nitrogen}} = \mu' \left(1 - \frac{k_Q}{Q} \right) \quad (13)$$

$$I = I_0 e^{-\lambda z} \quad (14)$$

$$Q = \frac{F}{C} \quad (15)$$

According to the threshold hypothesis only one factor is in control at any instant of time; the smaller growth rate is taken into the algorithm (Equation 11). Light-controlled growth rate is dependent on light intensity in each layer (Equation 12), which decreases exponentially with water depth (Equation 14). The daily mean light intensity at the sea surface in the observational region is estimated to be 80 W m^{-2} from the coastal regional meteorological stations. The nutrient-controlled growth rate (Equation 13) is determined by a function of the nutrient content in phytoplankton (Equation 15).

Nutrient uptake rate, c , is determined as independent of the factor controlling growth and given by

$$\gamma = \frac{\gamma_m D}{D_h + D} \quad (16)$$

This equation is a saturation function of the dissolved inorganic nitrogen.

The grazing rate, κ , and excretion rate, ϵ , are constant. To provide an input of new nutrient from upper layer of deep ocean to the bottom of the eddy, the flux is assumed by:

$$D_{\text{input}} = \frac{K_{z_{\text{bottom}}}}{\Delta z} D_{\text{flux}} \quad (17)$$

D_{flux} is a balance of the concentrations of dissolved inorganic nitrogen between the bottom layer of the eddy and the deep ocean. The concentration in the deep ocean is assumed to be $20 \mu\text{M}$.

Results

Hydrographic structure

Figure 4 shows the surface temperature and salinity distribution during the observational period. Temperature and salinity minimum along the Kuroshio front suggest the existence of upwelled water in the surface

layer. The vertical structure shown in Figure 5 indicates the eddy location most obviously by a cold water uplift at K11 shallower than 150 m. The location of the uplift corresponds to the location of the cyclonic eddy observed by the satellite and it is different from a peak at K12 deeper than 150 m associated with the Kuroshio front. This result indicates that the vertical scale of the upwelling caused by the eddy is of the order of 50–100 m.

Since the observations were spread over 6 days, the horizontal distributions will not represent the instantaneous hydrographic structure around the front. In addition, the small vertical scale of the eddy and surface heating make it difficult to identify a shape of the eddy from these figures. However, roughly estimated horizontal differences of temperature and salinity between the eddy region and surrounding water are about 2°C and 0.1 respectively. These values are used for the model.

Biological structure

Figure 6(a–c) shows the distribution of nitrate, phosphate and chlorophyll concentrations in the surface layer. Regions of high nutrient and chlorophyll concentrations are evident along the Kuroshio front. For convenience of further analysis, we put numerals on the cores of high nitrate concentration (Fig. 6a). The highest concentration of phosphate is in Core 1, slightly north of the high concentration of chlorophyll. Since the location of Core 1 corresponds to the location of the eddy, which has travelled half of a day from the eddy seen in Figure 2, it suggests that the high nutrients are supplied by upwelling within the eddy. According to the hydrographic observations, the water mass at Line 1 reaches Line 3 in two days. Temperature and salinity profiles at the centre of Core 1 (K4) correspond well to that at Core 2 (K17), particularly at depths less than 200 m, although those at the other stations on Line 1 and 3 spread over a wider range (Fig. 7). These results indicate that Core 2 water was that at Core 1 two days previously. In these two days the concentration of nitrate decreased from 6 to $3 \mu\text{M}$ and phosphate from 0.15 to $0.05 \mu\text{M}$, with the chlorophyll concentration increasing from $1.5 \text{ }\mu\text{g l}^{-1}$ to $2.5 \text{ }\mu\text{g l}^{-1}$ at the sea surface. We infer that phytoplankton growth has resulted in the consumption of $3 \mu\text{M}$ of nitrate and $0.1 \mu\text{M}$ phosphate. The nitrogen:phosphate ratio taken by the phytoplankton, 30:1, is slightly larger than the Redfield number.

Figure 8 shows vertical sections of nutrients and chlorophyll along Line 2. Nutrient structure along Line 2 is very similar to the hydrographic structure; peaks of both nutrients at K12 are recognized at depths greater than 200 m and those peaks at K11 are seen at depths less than 200 m. The location of K11 corresponds to the eddy location and it indicates that regional upwelling occurs inshore of the Kuroshio front. The location of

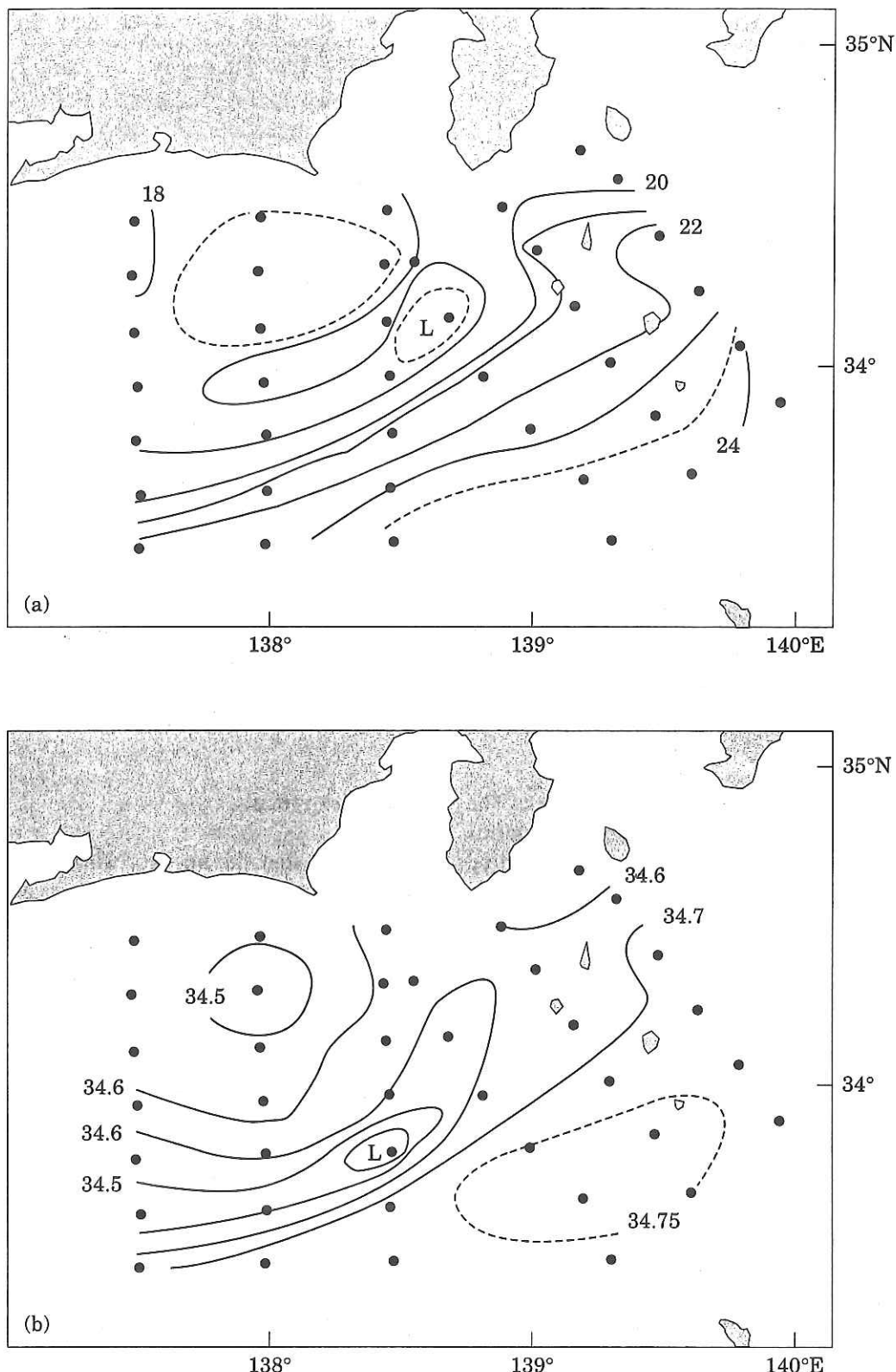


Figure 4. (a) Surface temperature ($^{\circ}\text{C}$) and (b) salinity distributions on 18–23 May, 1994.

high chlorophyll concentrations does not exactly correspond to that of high nutrients. However, considering that the contour of $1.0 \mu\text{g l}^{-1}$ is spread over neighbouring stations and that there is a time lag between the nutrient supply and consumption, the high concentrations are most probably associated. The vertical scale

of the high concentration of chlorophyll is about 50 m with a maximum at a depth of 30 m.

Primary production

In the cyclonic eddy, $3 \mu\text{M}$ of nitrate was consumed for production of phytoplankton, which is equivalent to

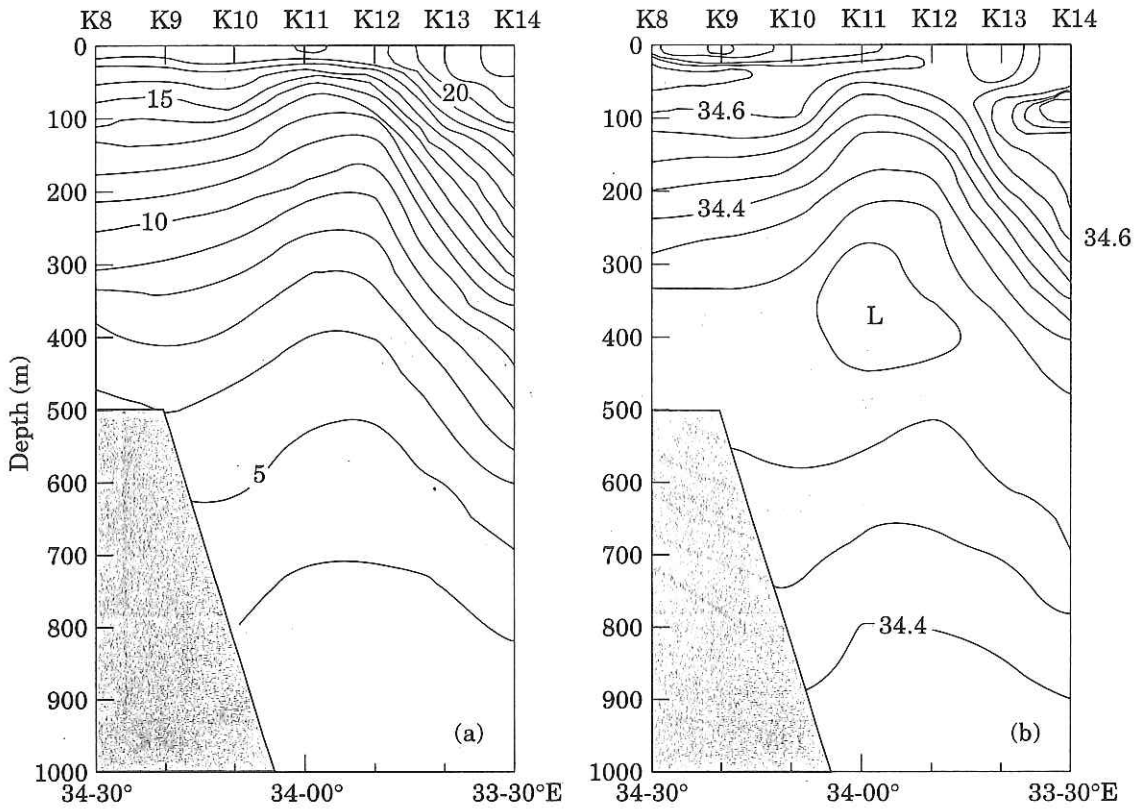


Figure 5. (a) Vertical temperature ($^{\circ}\text{C}$) and (b) salinity sections along Line 2.

$1.0 \mu\text{g l}^{-1}$ of chlorophyll during the two days. The apparent specific growth rate of phytoplankton in terms of chlorophyll was calculated assuming an exponential change, i.e.:

$$\mu' = 1/(t_2 - t_1) \ln c_2/c_1, \quad (18)$$

where c_1 and c_2 are the concentrations of chlorophyll at times t_1 and t_2 respectively. The apparent specific growth rate is estimated to be 0.26 d^{-1} . Supposing the chlorophyll:nitrogen ratio equals 0.7 (Ishizaka *et al.*, 1986), $3 \mu\text{M}$ decrease of nitrate indicates $4.3 \mu\text{g l}^{-1}$ chlorophyll production by phytoplankton. Since the chlorophyll concentration increased by only $1.0 \mu\text{g l}^{-1}$, we deduce that $3.3 \mu\text{g l}^{-1}$ chlorophyll was lost by sinking and zooplankton grazing during the two days.

Eddy vorticities on each observational line estimated from current velocity measured via the ADCP decrease with time: Line 1 $2.0 \times 10^{-5} \text{ s}^{-1}$, Line 2 $1.5 \times 10^{-5} \text{ s}^{-1}$, Line 3 $1.0 \times 10^{-5} \text{ s}^{-1}$. Since the eddy diameter is 80 km and the velocity difference between the centre of the eddy and the Kuroshio front is about 150 cm s^{-1} , the initial vorticity of the eddy is estimated to be $3.5 \times 10^{-5} \text{ s}^{-1}$. According to this estimation, the eddy is generated two days before Core 1. Supposing the initial concentration of surface nitrate is $8 \mu\text{M}$, because the vertical scale of the upwelling is 50–100 m, variation of nitrate can be explained by the following equation with t in days.

$$y = 12 - 4\exp(0.2t) \quad (19)$$

This implies that the nutrient will be consumed within 3–4 days from the Core 1. These paths are illustrated in Figure 9. This daily loss of the nutrients contributes towards the total primary production. The daily total chlorophyll concentration and the specific growth rate of phytoplankton, including grazing and sinking effects, can be estimated from the nutrient consumption and the apparent chlorophyll concentration. For instance, the apparent concentration of chlorophyll on the second day, $1.5 \mu\text{g l}^{-1}$, increases by $0.45 \mu\text{g l}^{-1}$ to $1.95 \mu\text{g l}^{-1}$ on the third day. However, since the nitrate concentration decreases by $1.33 \mu\text{M}$, corresponding to $1.9 \mu\text{g l}^{-1}$ chlorophyll concentration, actual concentration on the third day is estimated to be $3.40 \mu\text{g l}^{-1}$. The balance, $1.45 \mu\text{g l}^{-1}$, is lost by grazing and sinking in one day and the specific growth rate, 0.82 d^{-1} , is estimated. The average of the specific growth rate during the five days is 0.8 d^{-1} .

Modelling

According to the observations, the average temperature in the surface layer of the eddy is 2–3°C higher than the surrounding water. Surface temperature in the model is increased by about 2°C in 7 days as shown in Figure 10(a). This modelled increase of the temperature agrees well with the observations. Wind stress at the sea surface and bottom friction between the eddy bottom and upper

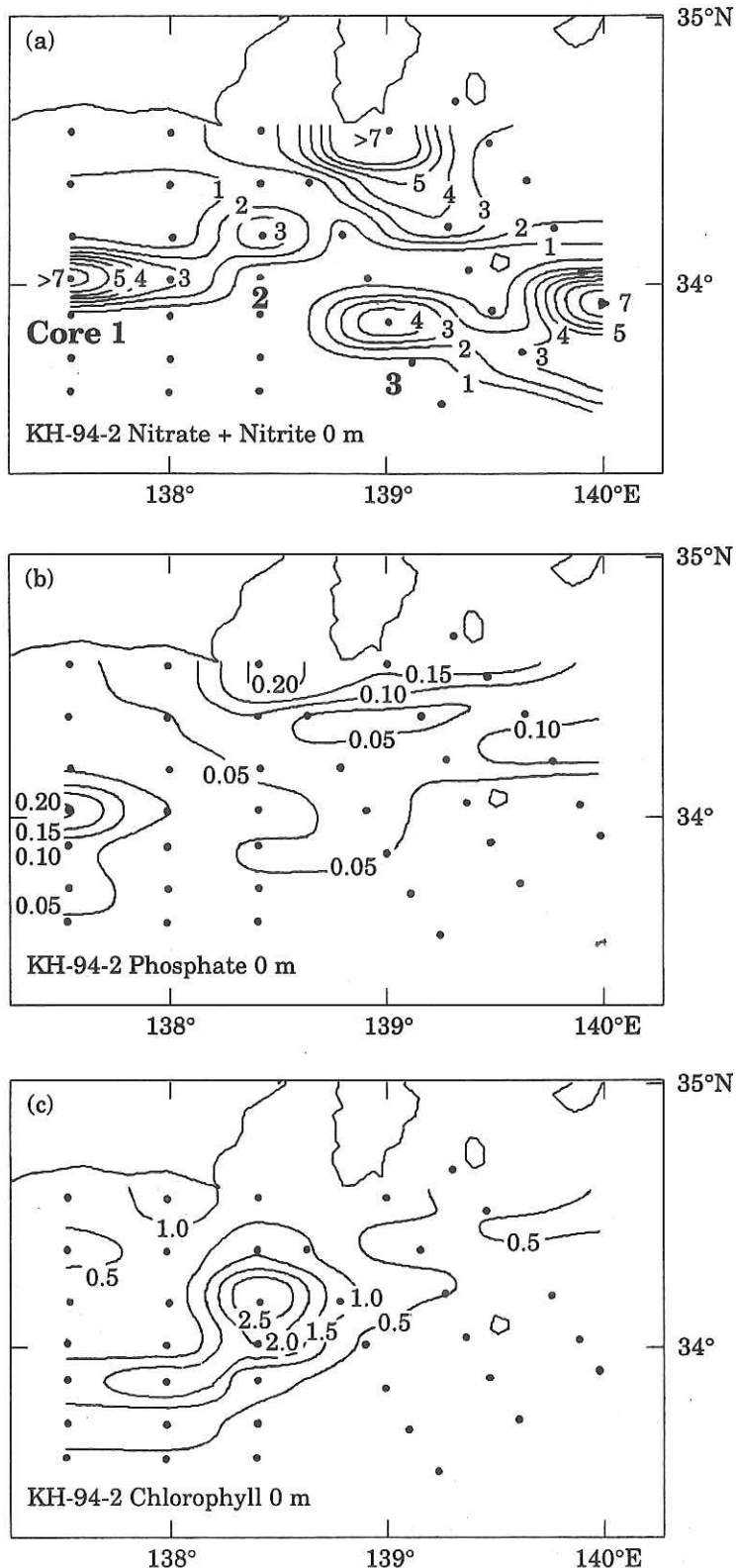


Figure 6. Surface distributions of nitrate (a), phosphate (b) and chlorophyll (c) concentrations. Units of nutrients and chlorophyll are μM and $\mu\text{g l}^{-1}$, respectively. Large figures in (a) indicate core number.

layer of the deep ocean cause vertical mixing. The modelled turbulent intensity is shown in Figure 10(b). The vertical mixing is dominant in the top 15 m of the

sea surface and a 30 m layer at the eddy bottom. The combination of mixing and surface heating produce weak stratification at a depth of 50 m.

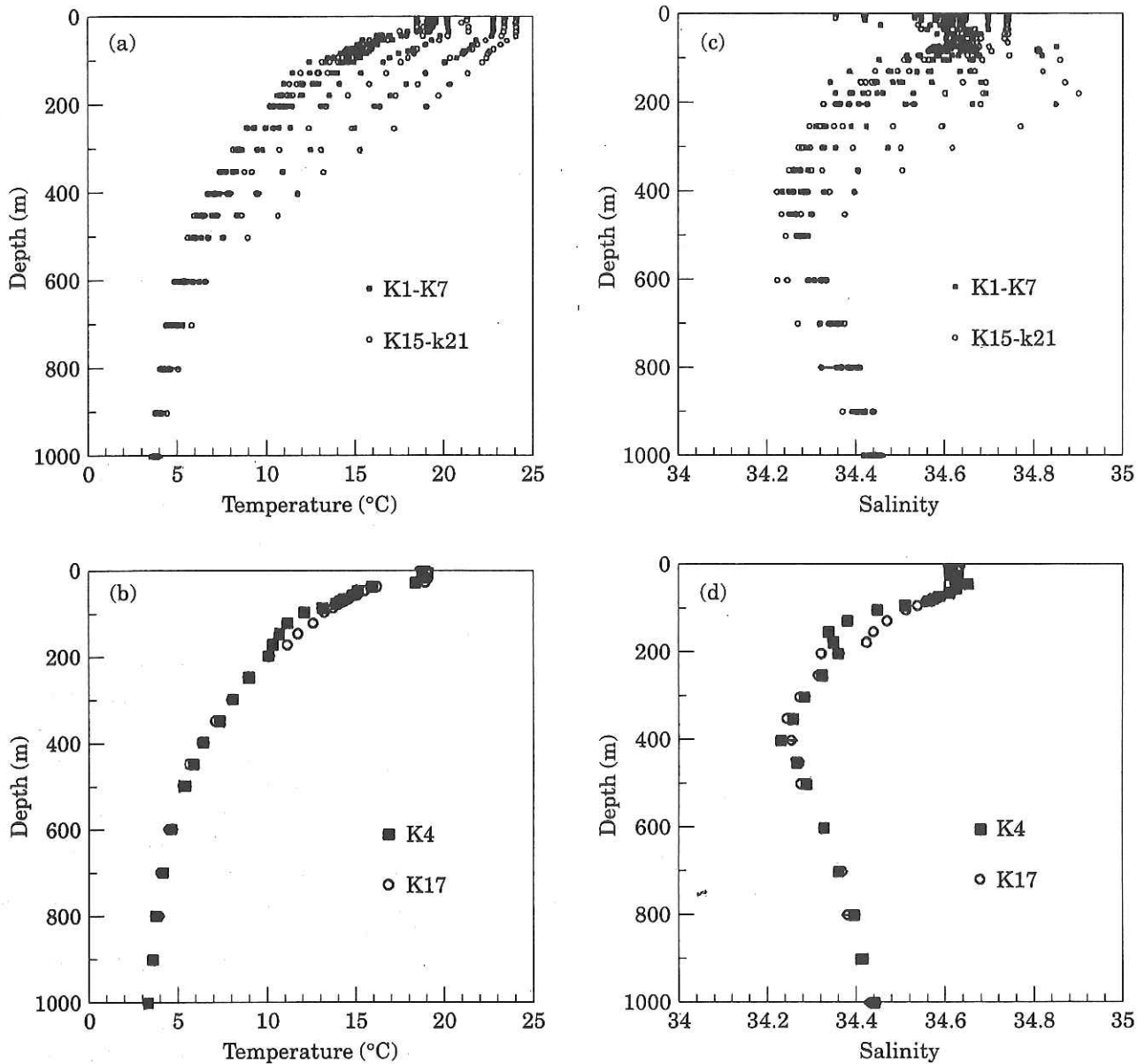


Figure 7. Temperature and salinity vertical profiles along Line 1 and 3.

Biological predictions from the model are shown in Figure 10(c-f). The concentration of chlorophyll reaches a maximum of $3.6 \mu\text{g l}^{-1}$ on the fifth day after the generation, when the dissolved inorganic nitrogen is almost exhausted. The time when the nutrients are exhausted and the chlorophyll concentration peaks correspond quite well to those shown in Figure 9. After the fifth day, the concentration of chlorophyll decreases rapidly because of the lack of nutrients. However, the nitrogen-in-plankton is at a maximum on the fourth day prior to the maximum of chlorophyll and the value has already decreased when the chlorophyll concentration is maximum.

A contour of $1.0 \mu\text{g l}^{-1}$ in the chlorophyll concentration always exists at a depth of 32 m throughout the calculation and its changes are restricted to depths

shallower than 30 m. Because it is associated with growth of phytoplankton the concentration of the dissolved inorganic nitrogen decreases markedly at depths shallower than 60 m. A concentration of $8.0 \mu\text{M}$ which existed in the sea surface at day 0 is found at a depth of 65 m on the seventh day. By this stage the surface concentration of dissolved inorganic nitrogen has reverted to what would be expected without the presence of the eddy.

The modelled growth rate shown in Figure 10(f) is similar to the specific growth rate estimated from the observational results. The high growth rates in excess of 0.8 d^{-1} are limited to depths less than 30 m until the fourth day. However, the depth of the maximum increases after that with decreases of the nitrogen-in-plankton.

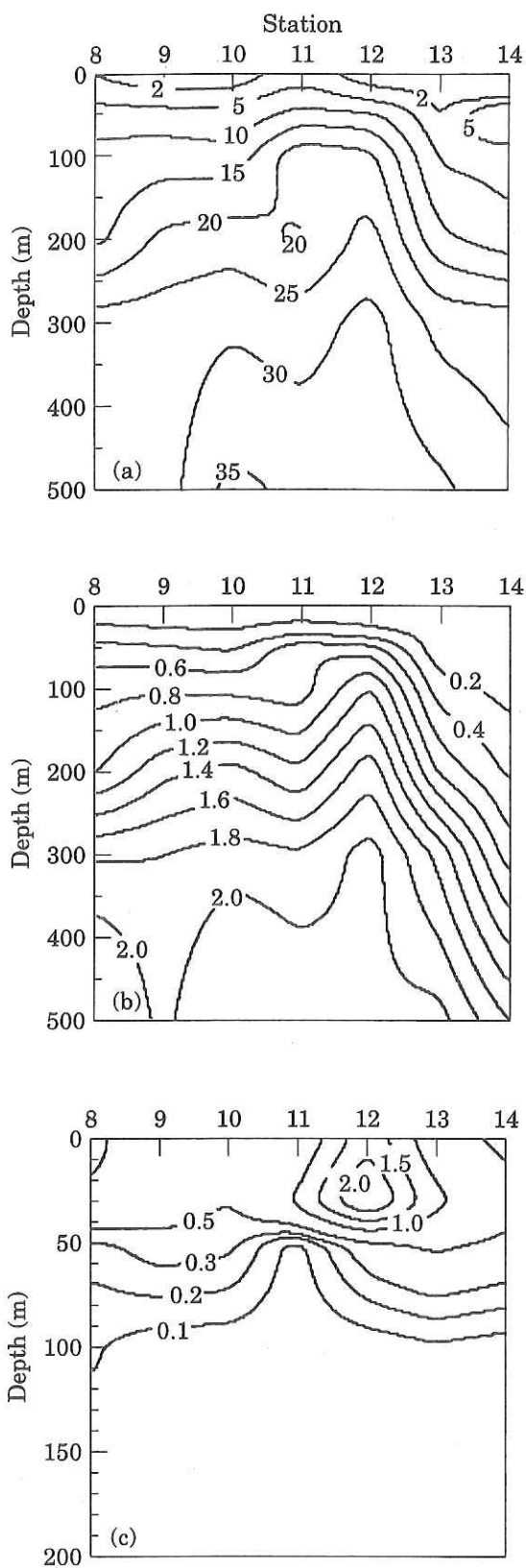


Figure 8. Vertical sections of nitrate (a), phosphate (b) and chlorophyll (c) concentrations along Line 2. Units of nutrients and chlorophyll are μM and $\mu\text{g l}^{-1}$, respectively.

Discussion

In this paper, we describe increased primary production caused by an eddy associated with frontal disturbances

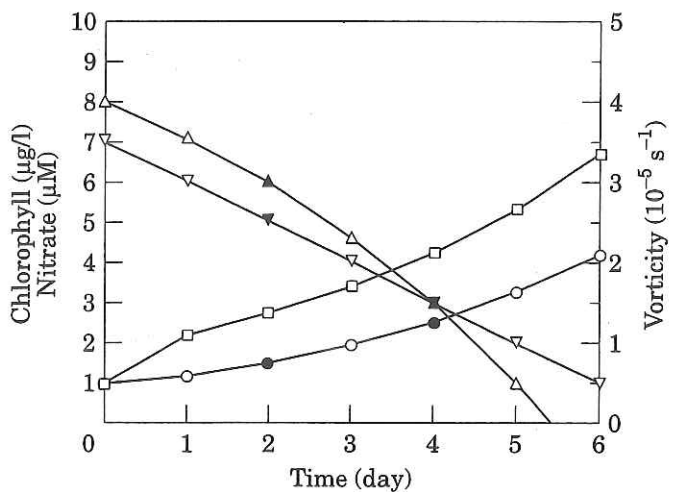


Figure 9. Variations of estimated physical and biological factors in the cyclonic eddy. The calculation is started from eddy generation. Data in Core 1 and 2 observed on the second and fourth day are indicated by solid symbols. ($-\Delta-$ nitrate, $-\circ-$ apparent chl., $-\square-$ total chl., $-\nabla-$ vorticity).

of the Kuroshio. After its generation the nutrient-enriched eddy detaches from the Kuroshio front and intrudes into the coastal area of the Enshu-nada Sea. According to our calculations the life span of the eddy is estimated to be 7 days from vorticity changes and 6 days from nutrient consumption. During this period, the apparent chlorophyll concentration in the eddy reached $3.3 \mu\text{g l}^{-1}$ on the fifth day after the generation, when the nutrient was exhausted and the vorticity of the eddy became less than $1 \times 10^{-5} \text{ s}^{-1}$. According to the model results, the specific growth rate of phytoplankton decreased rapidly after the maximum chlorophyll concentration was reached but was constant before the maximum. These results indicate that new production by upwelling in the eddy spread over the Enshu-nada Sea and contributed to the coastal primary production within about a week. The estimated values from observations correspond well to those from the numerical simulation.

A high concentration of chlorophyll is observed at depths less than 50 m with a maximum at 30 m. The high concentration calculated by the simulation is found at depths shallower than 30 m. The depth in the simulation is largely prescribed by the light-dependent growth rate, although stratification, resulting from mixing and heating, also contributes. In the model, a maximum in stratification at a depth of 50 m makes nutrient supply to the euphotic layer difficult. This is a reason why the chlorophyll maximum at the depth of 30 m was not reproduced in the model. A high growth rate is, however, modelled at depths of 30 m after the fourth day. This maximum is prescribed by a balance between light and nutrient dependent growth rates because the high concentration of nutrient has already been exhausted in the surface layer.

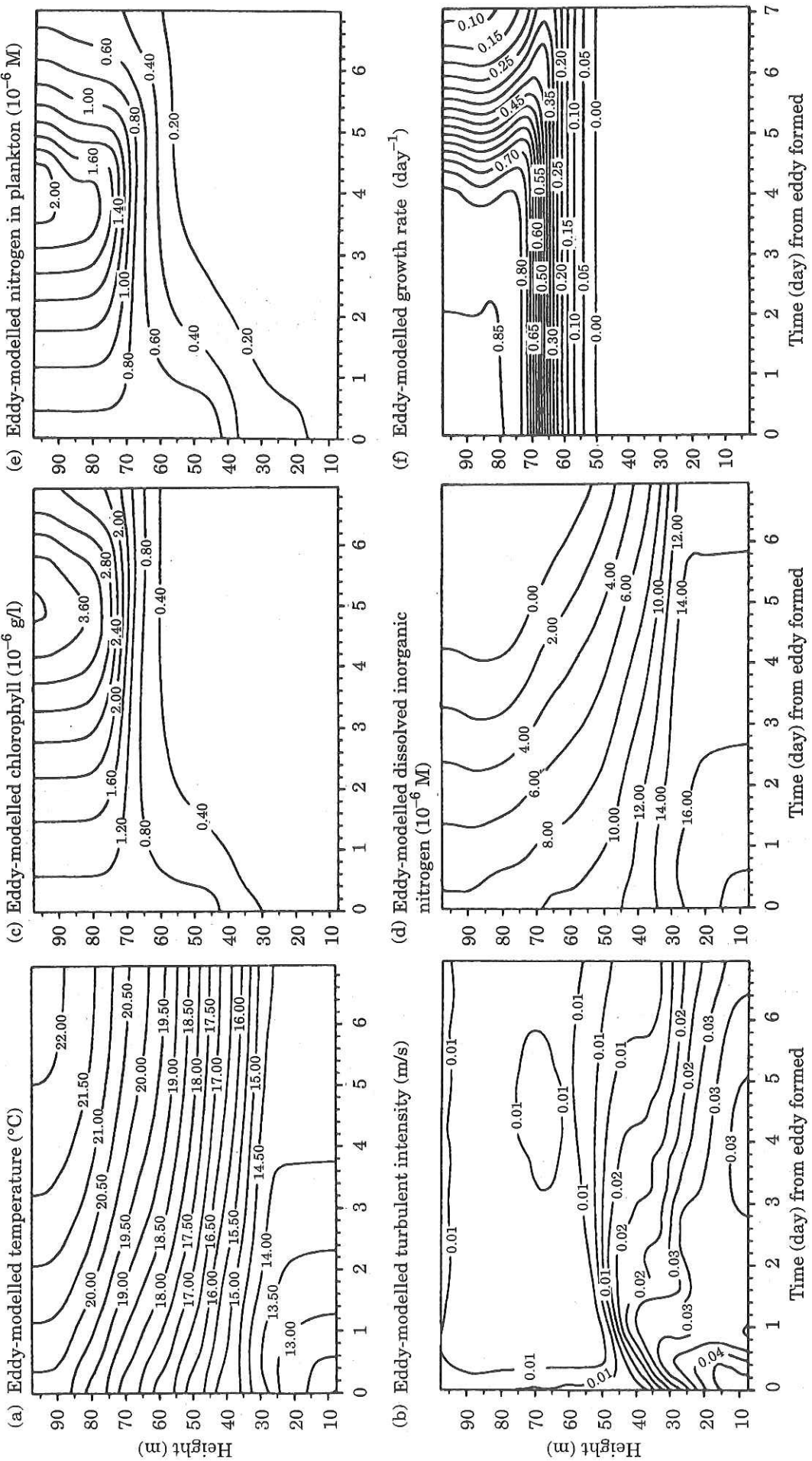


Figure 10. Modelled variations of (a) temperature, (b) turbulent intensity, (c) chlorophyll concentration, (d) concentration of dissolved inorganic nitrogen, (e) concentration of nitrogen in plankton and (f) growth rate of phytoplankton.

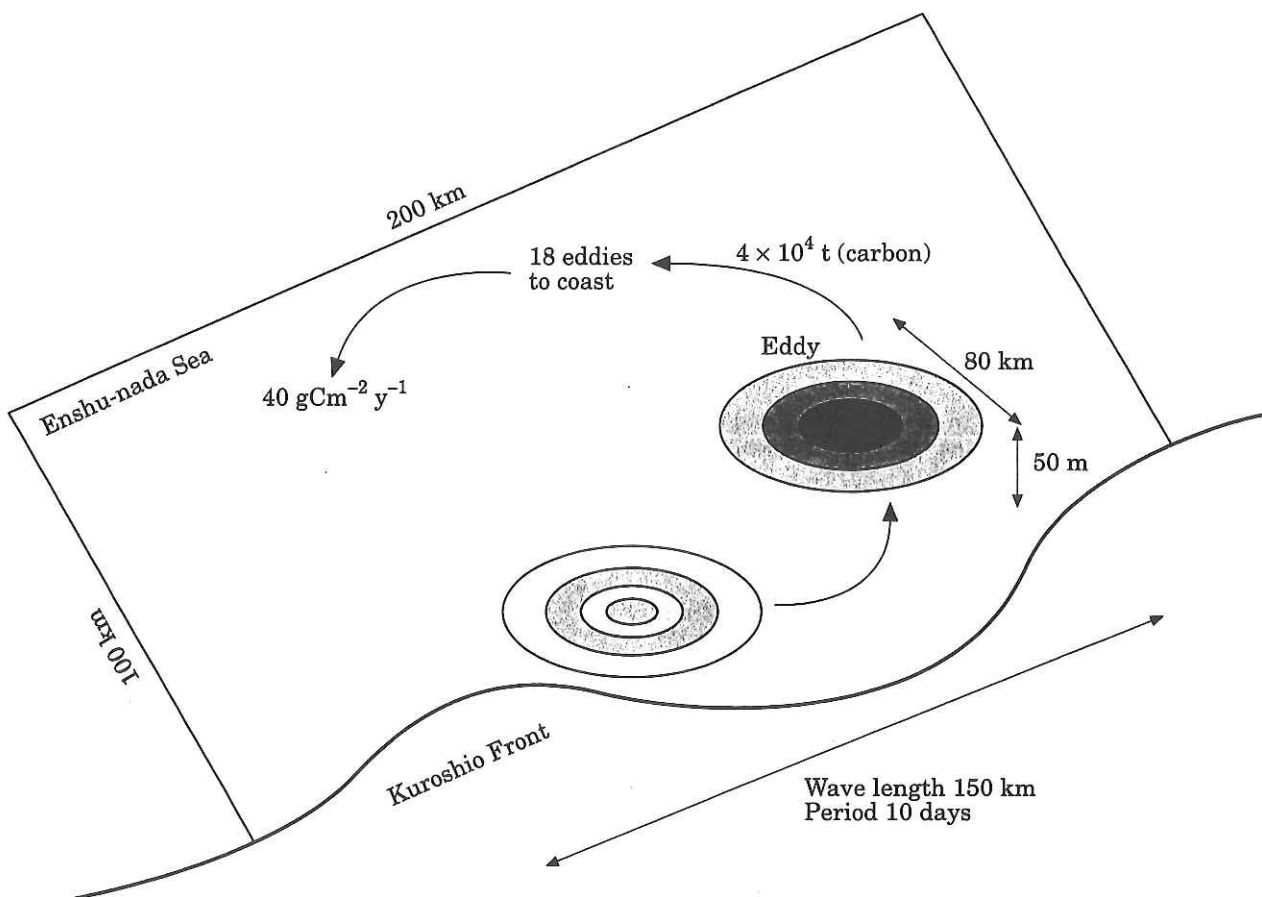


Figure 11. Schematic view of the Kuroshio front with diagrams of primary production.

The net primary production per litre in the eddy, including losses by grazing and sinking, is estimated to be 12.3 µg of chlorophyll over 6 days which is the period of the life of the eddy based on the initial surface nitrate concentration. Assuming the eddy has 80 km diameter and 50 m depth, and that the concentration becomes lower linearly from the centre of the eddy to the edge, the input of chlorophyll to the coast by one eddy would be 1.4 × 10⁹ g. Using a value of 30 for the carbon:chlorophyll ratio (Parsons *et al.*, 1984), we find a net production of 4.2 × 10¹⁰ gC. From satellite imagery, the frontal disturbance has a wavelength of about 150 km. In the Kuroshio region east of Cape Shionomisaki, a disturbance with this wavelength occurs every 10 days (Kimura and Sugimoto, 1993): 36 eddies a year. The impact of the net onshore flux of nitrate on phytoplankton production can, therefore, be estimated knowing the area influenced by the disturbances. However, since vertical mixing in winter enhances the nutrient supply to the euphotic layer, only the 18 eddies in summer, when stratification is developed, should be considered. Assuming 18 eddies intrude into the Enshu-nada Sea, which has an area of 100 km × 200 km, this perturbation could result in a carbon production rate of 40 gC m⁻² y⁻¹ (Fig. 11).

No precise estimation of primary production in the Enshu-nada Sea has ever been made. However, according to a rough estimation by Ichimura (1965), primary production in the coastal area and in an area between the coastal area and the Kuroshio front are 110–180 and 40–70 gC m⁻² y⁻¹ respectively. The primary production by the frontal disturbance, therefore, appears to account for a large part of coastal primary production. In fact, high densities of copepod nauplii seem to correspond with high chlorophyll concentration in the eddy, suggesting that it is important to understand the survival processes of the higher food web. Moreover this estimate is similar to an estimate of production at the Gulf Stream front; 32–64 gC m⁻² y⁻¹ (Lee *et al.*, 1981) and we believe this to be the first time a comparison between the Kuroshio and the Gulf Stream has been made in regard to primary production caused by frontal disturbances.

Acknowledgements

We would like to express our gratitude to Dr T. P. Rippeth, University of Wales, Bangor, for his discussions and English correction. We also wish to express our thanks to the captain and crews of the R/V *Hakuho-maru* of Ocean Research Institute, University of Tokyo.

References

- Bane, J., and Brooks, D. 1979. Gulf stream meanders along the continental margin from the Florida Straits to Cape Hatteras. *Geophysical Research Letters*, 6: 280–282.
- Edinger, J. E., Duttweiler, D. W., and Geyer, J. C. 1968. The response of water temperatures to meteorological conditions. *Water Resources Research*, 4: 1137–1145.
- Ichimura, S. 1965. A short review on primary production in the Kuroshio. *Bulletin Planktology in Japan*, 12: 1–6.
- Ishizaka, J., Takahashi, M., and Ichimura, S. 1986. Changes in the growth rate of phytoplankton in a local upwelling around the Izu Peninsula, Japan in May 1982. *Journal of Plankton Research*, 8: 169–181.
- Lee, T., Atkinson, L., and Legeckis, R. 1981. Observations of a Gulf Stream frontal eddy on the Georgia continental shelf, April 1977. *Deep-Sea Research* 28: 347–378.
- Legeckis, R. 1979. Satellite observations of the influence of bottom topography on the seaward deflection of the Gulf Stream of Charleston, South Carolina. *Journal of Physical Oceanography*, 9: 483–497.
- Kimura, S., and Sugimoto, T. 1993. Short-period fluctuations in meander of the Kuroshio path off Cape Shionomisaki. *Journal of Geophysical Research*, 98: 2407–2418.
- Mellor, G. L., and Yamada, T. 1982. Development of a turbulent closure model for geophysical fluid problems. *Reviews of Geophysics and Space Physics*, 20: 851–875.
- Parsons, T., Takahashi, M., and Hargrave, B. 1984. *Biological Oceanographic Processes*. 3rd edn. pp. 330. Pergamon Press, Oxford.
- Simpson, J., and Bowers, D. G. 1984. The role of tidal stirring in controlling the seasonal heat cycle in shelf seas. *Annales Geophysicae*, 2: 411–416.
- Simpson, J., Crawford, W., Rippeth, T. P., Campbell, A. R., and Cheok, J. V. S. 1996. The vertical structure of turbulent dissipation in shelf seas. *Journal of Physical Oceanography*, 26: 1579–1590.
- Tett, P., Edwards, A., and Jones, K. 1986. A model for the growth of shelf-sea phytoplankton in summer. *Estuarine, Coastal and Shelf Science*, 23: 641–672.
- Yoder, J., Atkinson, L., Lee, T., Kim, H., and McLain, C. 1981. Role of Gulf Stream frontal eddies informing phytoplankton patches on the outer southeast shelf. *Limnology and Oceanography*, 26: 1103–1110.

Implications of meso-scale eddies caused by frontal disturbances of the Kuroshio Current for anchovy recruitment

Hideaki Nakata, Shingo Kimura, Yuji Okazaki, and Akihide Kasai



Nakata, H., Kimura, S., Okazaki, Y., and Kasai, A. 2000. Implications of meso-scale eddies caused by frontal disturbances of the Kuroshio Current for anchovy recruitment. – ICES Journal of Marine Science, 57: 143–152.

This paper discusses the implications of the meso-scale eddies, which are caused by frontal disturbances of the Kuroshio Current, for larval transport, distribution and food availability for Japanese anchovy, *Engraulis japonicus* (Houttuyn). It is a ubiquitous feature of the Kuroshio Front that wave-like meanders, with wavelengths of 100–400 km, generate cyclonic frontal eddies off the Pacific coast of the island of Japan. These eddies are likely to affect larval transport and the survival of the coastal spawning fish such as anchovy in the Kuroshio region by possibly moving coastal water offshore to the frontal region.

With this in mind, a frontal eddy was tracked from 18–23 May 1994 in the Enshu-nada Sea, where one of large spawning grounds of anchovy was found. Intensive transect surveys across the eddy were made to collect anchovy eggs and larvae simultaneously with prey organisms e.g. naupliar and copepodite copepods. These surveys showed that anchovy eggs and larvae hatched in the coastal water of the Enshu-nada Sea were entrained into the frontal eddy and transported along the Kuroshio Front, possibly recruiting to coastal nurseries in the Enshu-nada Sea. In addition, the upwelling of nutrient-rich water in the vicinity of this cyclonic eddy enhanced primary production and subsequent copepod production, providing potentially favourable conditions for the feeding and growth of the anchovy larvae entrained in the eddy.

© 2000 International Council for the Exploration of the Sea

Key words: anchovy recruitment, egg and larval entrainment, frontal eddy, Kuroshio Current.

Received 12 October 1998; accepted 4 December 1999.

H. Nakata, S. Kimura, and Y. Okazaki: Ocean Research Institute, University of Tokyo, 1-15-1 Minamidai, Nakano, Tokyo 164-8639, Japan. A. Kasai: Department of Fisheries, Faculty of Agriculture, Kyoto University, Oiwake, Kitashirakawa, Sakyo, Kyoto 606-8502, Japan.

Introduction

Most small pelagic fishes such as sardine and anchovy in and around Japan have their spawning grounds in the Kuroshio and its coastal water. Consequently, whether or not eggs and larvae are transported to the nurseries by the Kuroshio Current has been seen as a critical factor affecting larval survival and subsequent recruitment. In fact it was suggested that a large-scale meander of the Kuroshio Current could be related to marked fluctuation of the fish stocks (Watanabe, 1982), although the cause–effect relationship has not yet been clarified. In recent years, on the other hand, it has been revealed by detailed analyses of ocean fine-structure using satellite imagery that meso-scale eddies caused by

frontal disturbances (“frontal eddies” hereafter) are a ubiquitous feature along the coastal edge of the Kuroshio Current. It has also been suggested that those frontal eddies could play an important role in primary production due to the upwelling of nutrient-rich deep water to the surface euphotic zone, as a result of the cyclonic motion of the eddy (Lee *et al.*, 1981; Yoder *et al.*, 1981; Sasaki *et al.*, 1985; Kimura *et al.*, 1997). According to Kimura *et al.* (1997), total annual nitrogen input to the Enshu-nada Sea by the frontal eddies could result in a carbon production rate of $40 \text{ gCm}^{-2} \text{ y}^{-1}$, which is almost equivalent to the production rate estimated for the Gulf Stream frontal eddy (Lee *et al.*, 1981). This enrichment process possibly intensifies trophic level interactions (Haney, 1986; Bakun, 1996) and may affect

larval feeding and growth in the offshore frontal regions. To date, however, there has been only very limited information on this aspect.

In addition, Nakata (1992) suggested the possibility of entraining coastal low-salinity water by a frontal eddy to the Kuroshio Front in the southern continental shelf of the East China Sea. This entrainment could function as a mechanism of egg and larval transport from coastal spawning grounds offshore. Kidachi (1997), in fact, reported that aggregations of some inshore and coastal species of copepods such as *Acartia omorii* and *Calanus sinicus* were often observed in the vicinity of Kuroshio Front as narrow bands, suggesting that they accumulated at the Kuroshio Front under the influence of a frontal eddy. However any clear evidence for the egg and larval entrainment has not yet been demonstrated and there has been almost no consideration of the implication of the entrainment for the recruitment of coastal spawners.

In this paper we describe an intensive transect survey on the distribution and food availability of anchovy larvae in relation to the formation and development of a frontal eddy observed in the Enshu-nada Sea. This is one of the major spawning grounds of the Pacific subpopulation of Japanese anchovy, *E. japonicus* (Houttuyn). Part of the data on the nutrients and chlorophyll *a* concentrations obtained from this survey have already been presented in Kimura *et al.* (1997); in this paper more attention is given to the data on anchovy larvae and their prey organisms (mainly naupliar copepods). The implication of the coastal water entrainment by the frontal eddy for anchovy recruitment is also discussed in relation to the larval transport and survival processes.

Description of the transect survey in the Enshu-nada Sea

In addition to hydrographic observations with a conductivity-temperature-depth profiler (CTD), which were carried out at 39 stations in the Enshu-nada Sea along six transects during 18–23 May 1994 (see Fig. 1 of Kimura *et al.*, 1997), fish eggs and larvae were collected by 3–5 min. horizontal tows with the Ocean Research Institute (ORI) net, made of 0.33 mm mesh filtering cloth (1.6 m in diameter), and by a 15-minute multi-layer tow at six depths (0, 20, 40, 60, 100, 200 m) with the Motoda (MTD) net, made of the same filtering cloth (0.56 m in diameter) at night along two of the six transects. Naupliar and copepodite copepods were also collected from the surface water (1 l) using a bucket simultaneously with the net tows. Fish eggs and larvae collected were immediately fixed in 2.5% seawater (v/v) gutaraldehyde, and copepod samples were fixed in 5% (v/v) seawater formalin after being concentrated by a plankton net with 0.020 mm mesh. Water samples for determining chlorophyll *a* concentration were taken

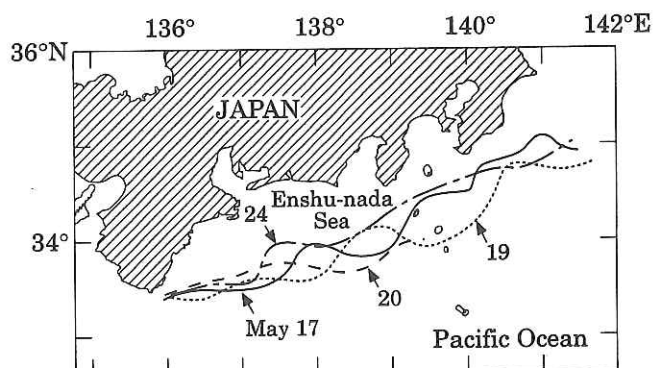


Figure 1. Variation in the Kuroshio Front during the period of observation (18–23 May 1994) in the Enshu-nada Sea off the central Pacific coast of Japan. The locations of the Kuroshio Front were detected using satellite images.

from 0, 30, 50 and 100 m depths along the same transects with Niskin bottles mounted on a rosette sampler attached to the CTD. The 200 cm³ of each water sample was filtered onto a Whatman GF/F glass microfibre filter and the filter soaked in 10 ml of dimethylformamide. The chlorophyll fluorescence in the dimethylformamide was later measured in the laboratory.

Since anchovy were predominant over the other fish species in the samples, the numbers of anchovy eggs and larvae were counted. In addition, for small catches (<50), all the anchovy larvae were measured to the nearest mm for total length (TL), and a random subsample was measured if the catch was larger than 50. These larvae were further grouped into 1 mm size classes, and ten individuals from each size class were homogenized for RNA and DNA analyses. The RNA and DNA contents were determined for each size class using a modification of the Schmidt-Thannhauser method (Buckley, 1979).

During the survey period, the Kuroshio Current took a straight path flowing close to the Japanese Pacific coast with small-scale meanders (Fig. 1). From the satellite image taken on 17 May 1994, a frontal eddy was clearly detected in the trough of the meander with 150 km horizontal wavelength, and apparently moved downstream of the Kuroshio Current at a speed of 60 cm s⁻¹ (Kimura *et al.*, 1997). The time-series of satellite images also showed that the intensity of the frontal eddy gradually decayed as it moved downstream. The horizontal distribution of sea surface temperature and salinity are shown together with the transects for egg and larval collection (SEC. I and SEC. II) in Figure 2. The main axis of the Kuroshio Current is indicated empirically by the 15°C isotherm at the depth of 200 m (Kawai, 1969), and the Kuroshio Front, which is marked with strong horizontal density gradient, forms a coastal boundary of the Kuroshio, being seen at the surface as the 20–21 isotherms and 34.6–34.7 isohalines in this survey. The elongated low temperature zone in

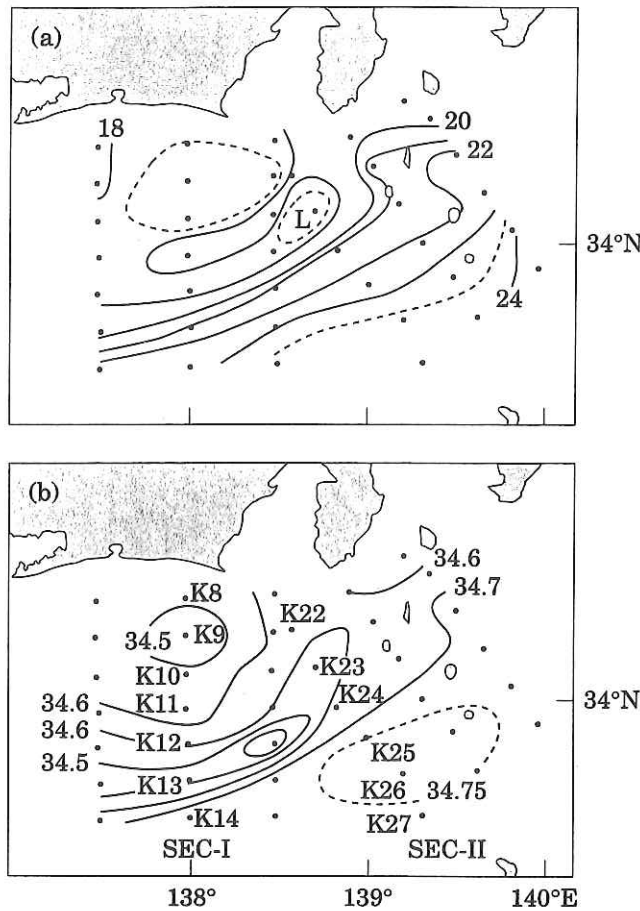


Figure 2. Distribution of sea surface temperature ($^{\circ}\text{C}$) (a) and salinity (b) obtained from a CTD survey in the Enshu-nada Sea. Transects for egg and larval collection and water sampling are shown in the lower figure together with the salinity distribution (SEC. I: Stns. K8–K14, SEC. II: Stns. K22–K27).

the northern edge of the Kuroshio Front as seen in Figure 2 indicates the existence of a cyclonic eddy and its eastward movement. Figure 3 further shows vertical temperature structure along SEC. I (K8–K14) and SEC. II (K22–K27). The Kuroshio Front was located between K12 and K13 in SEC. I and around K24 in SEC. II, and the frontal eddy was clearly indicated by convexed pattern of isotherms around K11–K12, corresponding with upwelling induced by the cyclonic eddy. The upwelling feature could not be seen in SEC. II, probably because, on the one hand, this transect did not pass through the centre of the eddy and, on the other, because of its decay with time (SEC. II was observed about 3 d after the transect survey along SEC. I). Nonetheless, we believe that Station K23 was located in the vicinity of the eddy centre.

Figure 4 shows the near-surface current field measured by a ship-board ADCP during the transect survey. Although this is a composite picture based on the data taken for several days (18–23 May 1994), it is evident that a cyclonic eddy was generated on the northern, colder edge of the Kuroshio Front. The maximum speed of the Kuroshio reached about 150 cm s^{-1} ,

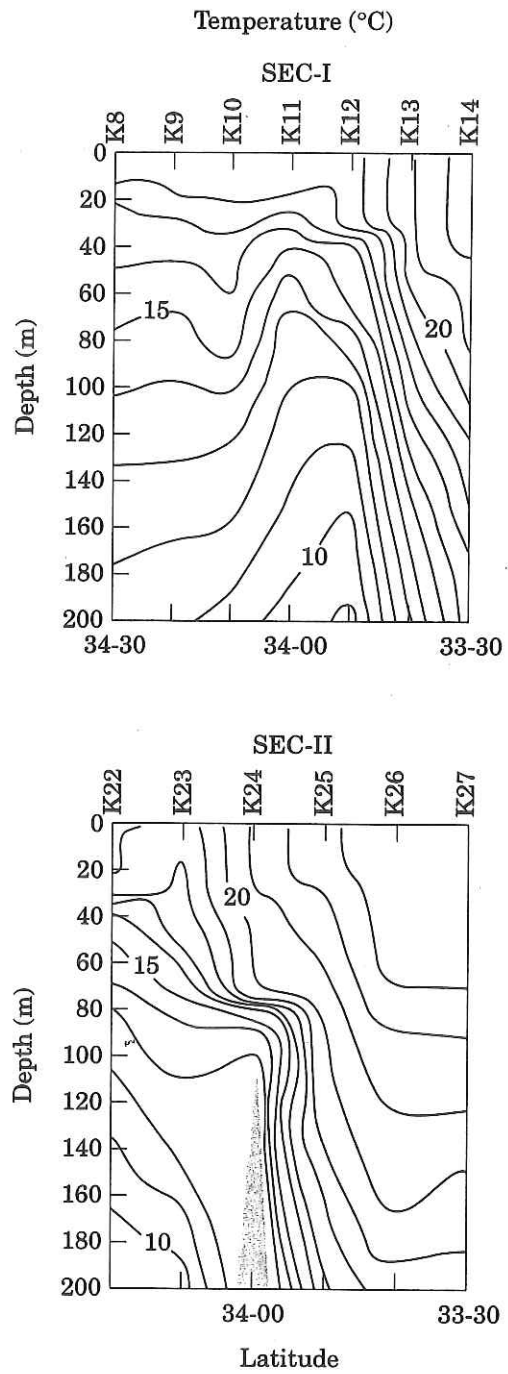


Figure 3. Vertical sections of temperature along SEC. I (top) and SEC. II (bottom) in the upper water of the Enshu-nada Sea.

while the eastward current velocities near the cyclonic eddy were of the order of $50\text{--}70 \text{ cm s}^{-1}$.

Results

Spatial distribution of fish larvae collected by a surface horizontal tow with the ORI net along SEC. I and SEC. II are shown together with spatial changes in the surface seawater temperature in Figure 5. Japanese anchovy with a size range of 2–20 mm TL predominated in the larval collection. Anchovy larvae were abundant in the

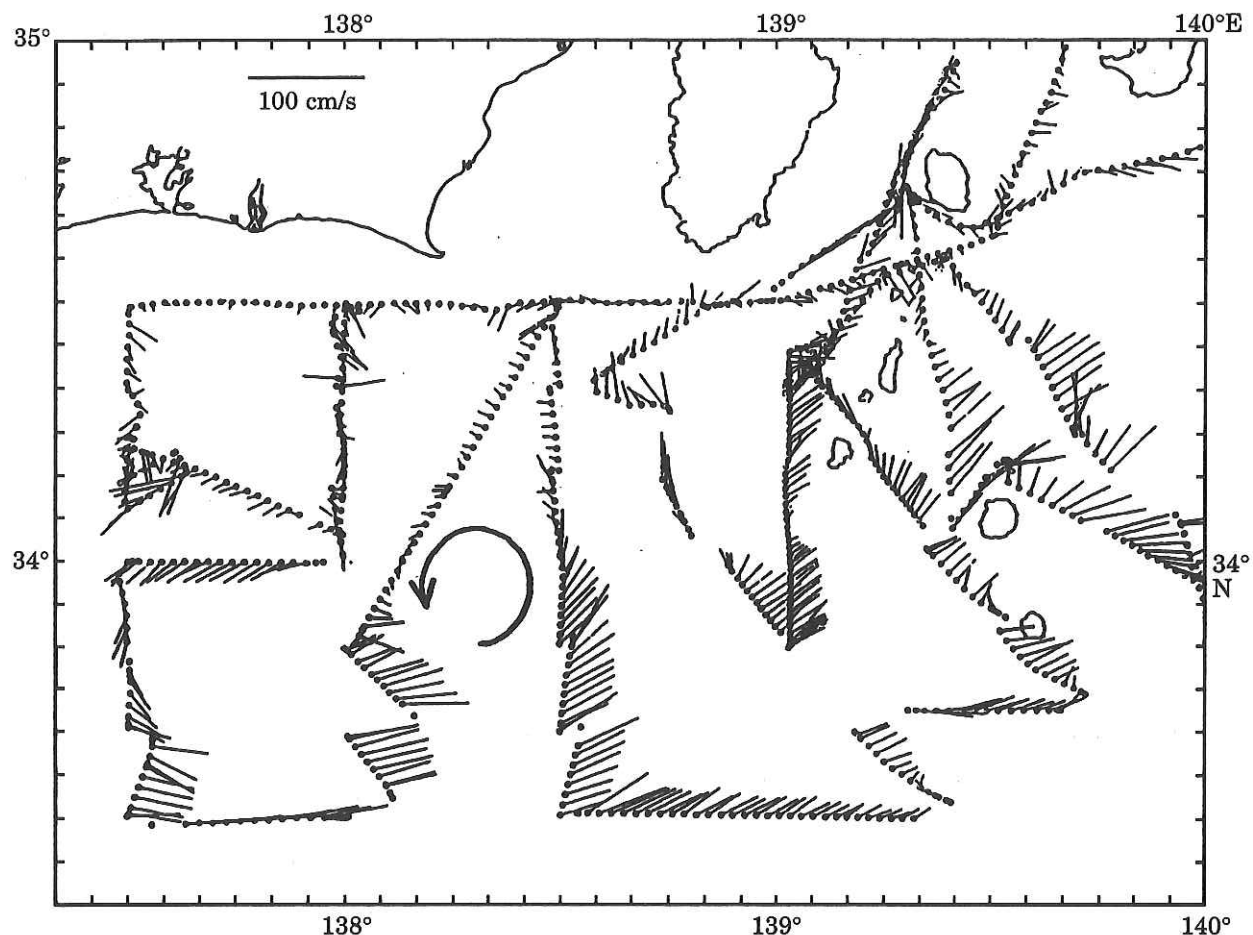


Figure 4. Distribution of the surface current measured by a ship-board ADCP during the survey period (18–23 May 1994).

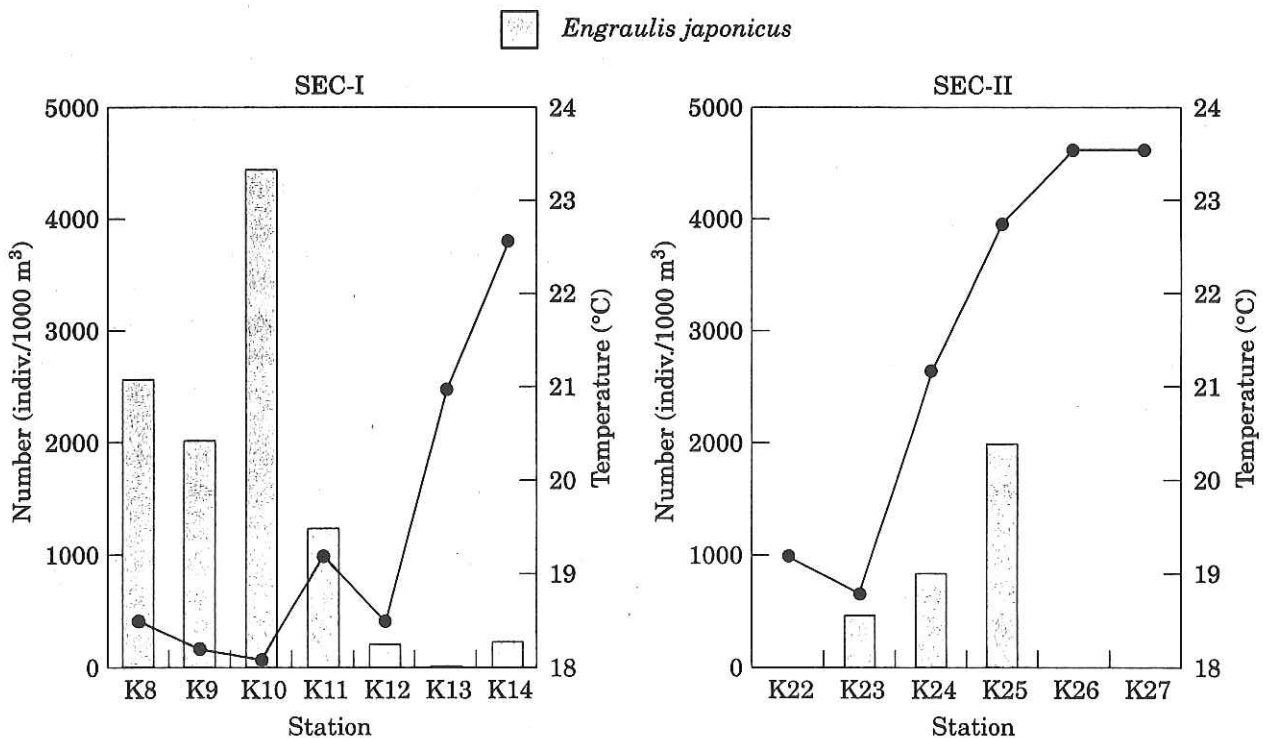


Figure 5. Spatial changes in the abundance of anchovy larvae (shadowed sticks) and sea surface temperature (solid lines) along SEC. I and SEC. II.

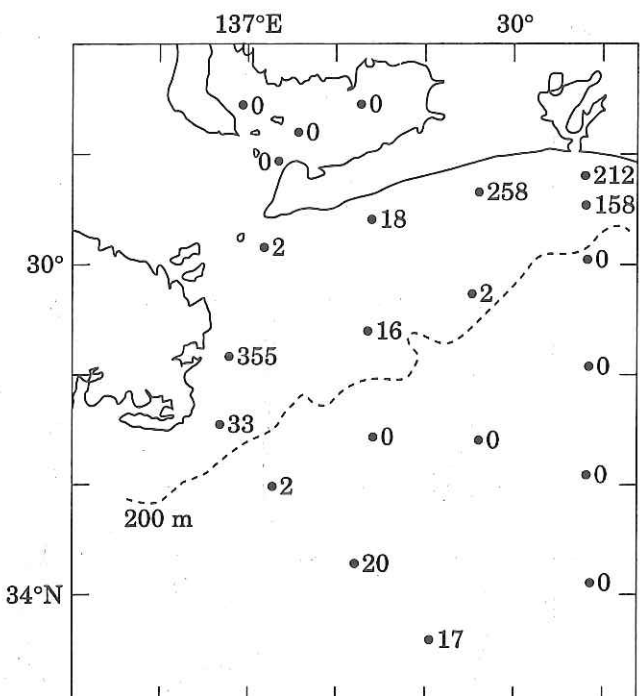
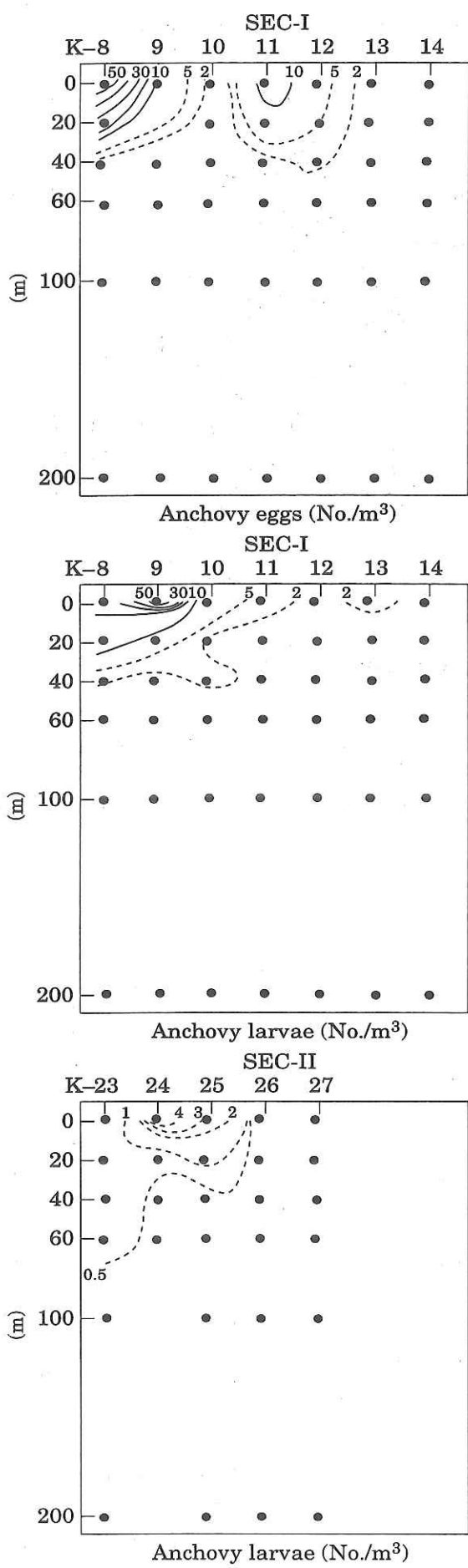


Figure 7. Horizontal distribution of anchovy eggs in the western Enshu-nada Sea on 10–11 May 1994. Numerals indicate the number of eggs per haul. Data from the Aichi Fisheries Research Institute.

coastal water just north to the Kuroshio Front along SEC. I, while they were more abundant in the Kuroshio Front itself along SEC. II. The same spatial distribution patterns were obtained from the larval collection with the MTD net as shown in Figure 6, although there was no sampling at Stn. K22 because of strong winds. It can also be seen from the vertical sections that most of anchovy larvae were vertically distributed in the surface layers (0–40 m). On the other hand, as shown in the top panel of Figure 6, anchovy eggs were most abundant in the surface water of the coastal station (K8) consistent with horizontal egg distribution in the surface water of the western Enshu-nada Sea on 10–11 May (Fig. 7). In addition a small peak of the egg density was observed at the eddy site (K11–K12 of SEC. I) near the Kuroshio Front. These imply that anchovy eggs and larvae originating from the coastal water were possibly entrained and moved to the offshore frontal region under the influence of the frontal eddy.

Most of the anchovy larvae collected in the coastal stations (K8 and K9) of SEC. I were less than 5 mm in length, while the 5 mm length class predominated at the eddy station (K23) of SEC. II. The upper panel of Figure 8 shows the frequency distribution of total length

Figure 6. Distributions of anchovy eggs along SEC. I (top), anchovy larvae along SEC. I (center), and anchovy larvae along SEC. II (bottom). The eggs and larvae were collected by a multi-layer tows with the MTD net (see the text for details).

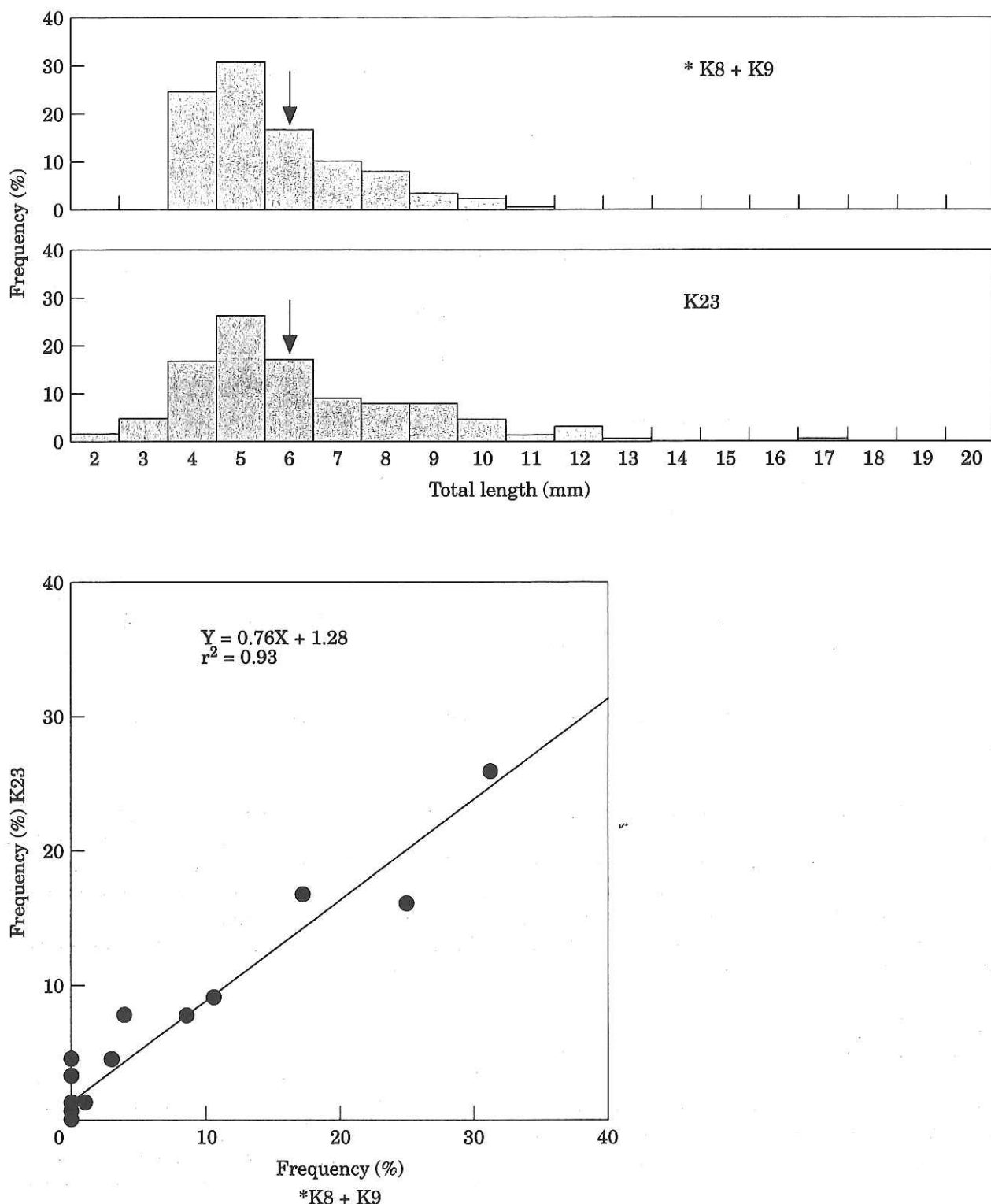


Figure 8. Correlation between the length frequency distributions of the anchovy larvae collected at Stn. K23 of SEC. II and Stns. K8 and K9 of SEC. I (lower panel). The upper panel shows the length frequency distributions at these stations. *The lengths of the larvae collected at Stns. K8 and K9 were transformed to those at three days after the collection, taking daily growth into account.

of anchovy larvae collected at K23 of SEC. II compared with that collected at K8 and K9 of SEC. I, after transformation of the latter to the probable distribution at three days after the collection, assuming a daily growth rate of the larvae in the coastal stations of

0.69 mm d^{-1} (Tsuji, 1985). As shown in the lower panel of Figure 8, the size composition of the eddy station in SEC. II apparently has a significant positive correlation with that of the coastal stations (K8 and K9) in SEC. I. This again supports the idea that the frontal eddy could

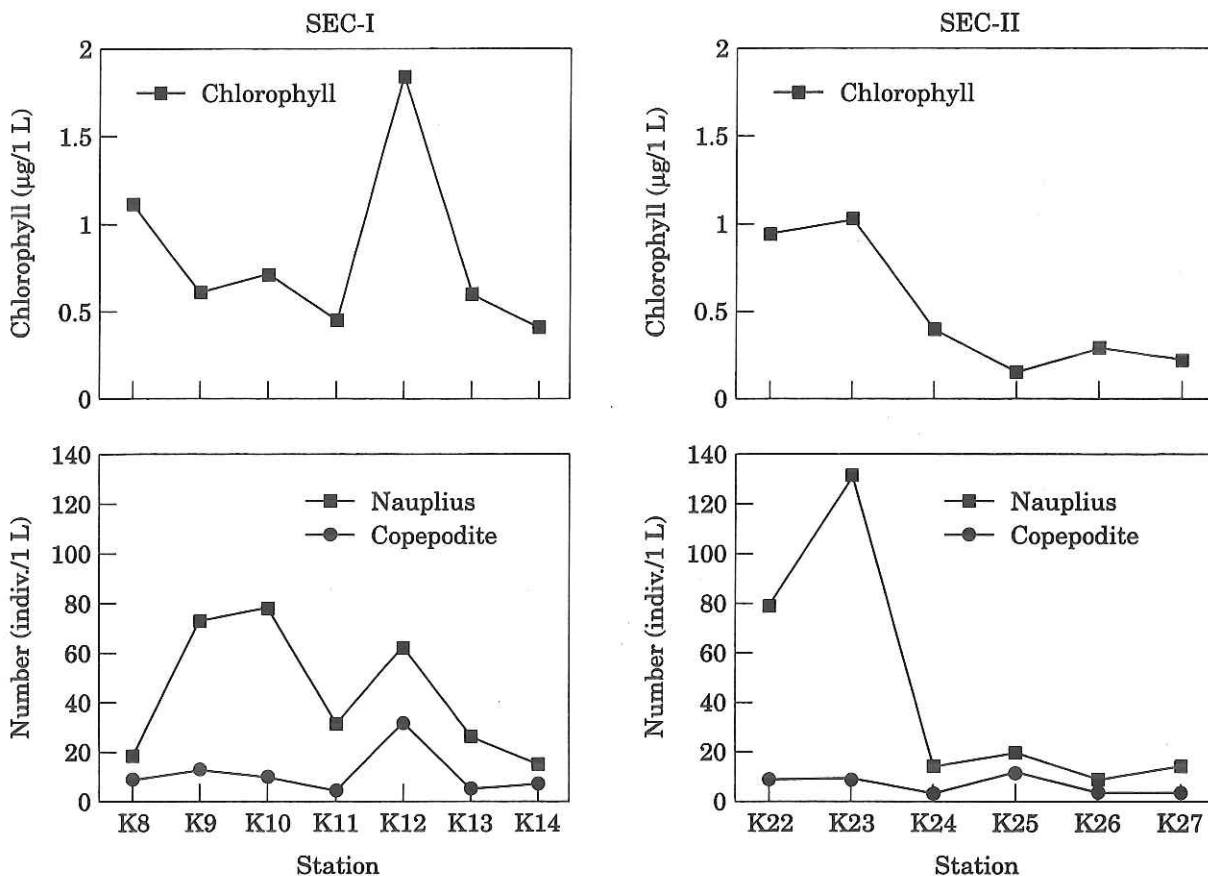


Figure 9. Spatial changes in the chlorophyll concentration and abundance of naupliar and copepodite copepods along SEC. I (left) and SEC. II (right).

entrain coastal anchovy larvae and carry them to the offshore frontal region trapped in an eddy.

Figure 9 further shows the spatial changes in chlorophyll *a* concentration and copepod abundance in the surface water along SEC. I and SEC. II. It is noticeable that a higher concentration of chlorophyll *a* was found at eddy station (K12) in SEC. I, while a marked increase in nauplius abundance was subsequently observed at eddy station (K23) in SEC. II. In the Kuroshio Front and its offshore stations, on the other hand, chlorophyll *a* concentration and copepod abundance were quite low. This suggests that the high chlorophyll *a* concentration at the eddy station may have stemmed from the upwelling associated with the eddy (Kimura *et al.*, 1997) promoting copepod production and leading to potentially enhanced food availability for the entrained anchovy larvae.

Regarding Stn. K12 in the SEC. I and Stn. K23 in the SEC. II as a region under the strong influence of the frontal eddy, all the stations were divided into three regions: inshore, frontal eddy and offshore, and the spatial difference in the RNA/DNA ratios of anchovy larvae for the size classes of 6–8 mm and for those of 9–11 mm in these three regions were studied. A significant increase (3.04 ± 0.24) was found in the frontal eddy compared to the inshore (2.51 ± 0.19) and offshore

(2.61 ± 0.22) for smaller size classes (6–8 mm) (Scheffe Test, $p < 0.05$), indicating that the overall nutritional condition of the early-stage larvae collected from the eddy site was better than those collected from the surrounding water. This difference between the frontal eddy and the other regions was not found with the larger size classes.

Discussion

One of the major spawning grounds of anchovy during the survey period was located in the coastal water of the Enshu-nada Sea, for example around K8 in SEC. I (Fig. 6). It is evident from this study that some of the anchovy larvae originating from the coastal water are entrained in the offshore frontal region when they encounter a frontal eddy during the period of offshore drift and dispersion. Although there is not necessarily a strong case of larval entrainment, this does give support to numerical simulation of shelf water entrainment into the Kuroshio Front by a topographic eddy, which is produced in association with onshore–offshore movement of the Kuroshio (Awaji *et al.*, 1991). Lagrangian measurement of the entraining process using drifter tracking in conjunction with egg and larval collection in the vicinity of the Kuroshio Front would be a way

of studying the eddy entrainment function of larval transport in more detail.

What are the implications of such an entrainment process for anchovy recruitment in the Enshu-nada Sea? Firstly there is enhanced food availability due to upwelling of nutrient-rich deep water in the vicinity of the frontal eddy and subsequent acceleration of primary production. As was shown in Figure 9, the abundance of copepod nauplii was doubled at the eddy site from the first to the second set of observations. Toda (1989) shows from a case study of regional upwelling near Izu Islands located in the east of the Enshu-nada Sea, that an increase in copepod egg production took place within a few days of the increase in food concentration. For the smaller copepods like *Paracalanus parvus*, one of the dominant copepod species in the Enshu-nada Sea (Kidachi, 1997; Nakata, unpublished data), the response time could be shorter (12–24 h at 18°C, Checkley, 1980a). Since nauplii generally hatch from the eggs within one day at around 20°C (Toda, 1989; Checkley, 1980b), marked increase in the abundance of copepod nauplii in the eddy site of SEC. II (Fig. 9) could be explained in this way.

Since sea surface temperature showed only a slight change at the eddy site (Stns. K12 and K23), copepod egg production was largely dependent of food concentration. According to Kimura *et al.* (1997), the maximum increase in chlorophyll *a* concentration estimated from the consumption rate of nitrate at the eddy site (Eq. 19 of Kimura *et al.* (1997)) could be 6.9 mg m⁻³ (from 1.5 mg m⁻³ on Day-2, when the first survey was made along the SEC. I, to 8.4 mg m⁻³ on Day-5, when the second survey was made along the SEC. II). Assuming that the egg production rate has a Michaelis-Menten relationship with the food concentration (Prestidge *et al.*, 1995), this increase in the chlorophyll *a* concentration from Day-2 to Day-5 could double the egg production rate, depending on the threshold and half-saturation phytoplankton concentrations for copepod grazing. Taking the case of *C. pacificus*, which has a threshold and half-saturation at 1.6 mg Chlm⁻³ and 4.0 mg Chlm⁻³, respectively (Runge, 1984), the egg production rate at Day-5 would be 1.7 times as large as that at Day-2.

Furthermore, a preliminary analysis of the nutritional condition of anchovy larvae showed that RNA/DNA ratios were appreciably higher for the larvae collected from the eddy stations compared to those collected from the surrounding stations. The spatial difference, however, was prominent only in the smaller size classes of less than 8 mm TL. This could result from the difference in morphological development, because anchovy larvae up to 8 mm TL after hatching have no fin-ray (Mitani, 1990). The development of the fin-rays must be indispensable to feeding and other active movements. It is obviously necessary in the future to track the same

eddy for a longer period (presumably for about one week according to Kimura *et al.*, 1997) to study in more detail the change with time in the nutritional condition of the larvae corresponding to elevated copepod production.

In addition, it should be noted in the macroplankton composition obtained simultaneously from the MTD net tows that the density of *Sagitta nagae*, that is well known as a predator of fish larvae (Funakoshi, 1992) was markedly high in the coastal water of SEC. I (Nakata, unpublished data), where anchovy eggs and small-sized larvae were concentrated. This suggests that entrainment by the frontal eddy may reduce the predation pressure from *S. nagae* and other coastal carnivorous plankton. This in itself will be beneficial to the anchovy recruitment if food availability is guaranteed.

In the coastal region of Enshu-nada Sea a westward current often develops whilst a cyclonic water circulation dominates the Sea overall. Kasai *et al.* (1993) for example, indicated that warm water intruded into the coastal region of Enshu-nada Sea intermittently with periods of about 50 and 20 days, both in association with the disturbances of the Kuroshio Current. Kimura and Sugimoto (1993), on the other hand, recognized 17–19-day period and 10–12-day period fluctuations in the small-scale meander of the Kuroshio Current, corresponding to the meander with a wavelength of 400 km and 200 km, respectively. This 10–20-day period is associated with the frontal disturbances of the Kuroshio and is closely related to the meso-scale feature described here, while the 50-day period is associated with a larger scale disturbance, such as local meandering of the Kuroshio path. The latter may drive the cyclonic circulation on the basin scale described above. Consequently, anchovy larvae once entrained by the frontal eddy would be transported downstream of the Kuroshio along the Kuroshio Front and then possibly move into the coastal region again in an intrusion of warm water with a larger temporal and spatial scale. This entrainment-intrusion cycle may contribute to sustaining anchovy recruitment in the Enshu-nada Sea. In other words, the recruitment may depend on the extent of any deviation from this sustained situation brought about by a large-scale meander of the Kuroshio Current.

Acknowledgements

We would like to express our gratitude to Professor T. Sugimoto, University of Tokyo, for his discussion and the encouragement he gave us to proceed with this study. We also thank the captain and crew of the R/V *Hakuho-maru* of the Ocean Research Institute, University of Tokyo for their assistance in the field survey. This study was supported in part by a Grant in Aid for Scientific Research from the Ministry of Education, Science and Culture of Japan.

References

- Awaji, T., Akitomo, K., and Imasato, N. 1991. Numerical study of shelf water motion driven by the Kuroshio: barotropic model. *Journal of Physical Oceanography*, 21: 11–27.
- Bakun, A. 1997. Patterns in the Ocean, Ocean Processes and Marine Population Dynamics. California Sea Grant College System, National Oceanic and Atmospheric Administration, 323 pp.
- Buckley, L. J. 1979. Relationships between RNA-DNA ratio, prey density, and growth rate in Atlantic cod (*Gadus morhua*) larvae. *Journal of Fisheries Research Board of Canada*, 36: 1497–1502.
- Checkley, D. M. Jr 1980a. The egg production of a marine planktonic copepod in relation to its food supply: laboratory studies. *Limnology and Oceanography*, 25: 430–446.
- Checkley, D. M. Jr 1980b. Food limitation of egg production by a marine, planktonic copepod in the sea off southern California. *Limnology and Oceanography*, 25: 991–998.
- Funakoshi, S. 1992. Relationship between stock levels and the population structure of the Japanese anchovy. *Marine Behavioral Physiology*, 21: 1–84.
- Haney, C. 1986. Seabird affinities for Gulf Stream frontal eddies: Responses of mobile marine consumers to episodic upwelling. *Journal of Marine Research*, 44: 361–384.
- Kasai, A., Kimura, S., and Sugimoto, T. 1993. Warm water intrusion from the Kuroshio into the coastal areas south of Japan. *Journal of Oceanography*, 49: 607–624.
- Kawai, H. 1969. Statistical estimation of isotherms indicative of the Kuroshio axis. *Deep Sea Research*, 16: 109–115.
- Kidachi, T. 1997. Distributional ecology of macrozooplankton in the Kuroshio and its adjacent waters off Honshu, mainland of Japan. PhD Thesis, Tokyo University, Tokyo, Japan.
- Kimura, S., Kasai, A., Nakata, H., Sugimoto, T., Simpson, J. H., and Cheok, J. V. S. 1997. Biological productivity of meso-scale eddies caused by frontal disturbances in the Kuroshio. *ICES Journal of Marine Science*, 54: 179–192.
- Kimura, S., and Sugimoto, T. 1993. Short-period fluctuations in meander of the Kuroshio path off Cape Shionomisaki. *Journal of Geophysical Research*, 98: 2407–2418.
- Lee, T., Atkinson, L., and Legeckis, R. 1981. Observations of a Gulf Stream frontal eddy on the Georgia continental shelf, April 1977. *Deep-Sea Research*, 28: 347–378.
- Mitani, I. 1990. The biological studies on the larvae of Japanese anchovy, *Engraulis japonica* HOUTTUYN, in Sagami Bay. Special Report of the Kanagawa Prefectural Fishery Experimental Station, 5: 1–140.
- Nakata, H. 1992. Effect of the Kuroshio frontal eddies on egg and larval transport. *Kaiyo Monthly*, 24: 295–299.
- Prestidge, M. C., Harris, R. P., and Taylor, A. H. 1995. A modeling investigation of copepod egg production in Irish Sea. *ICES Journal of Marine Science*, 52: 693–703.
- Runge, J. A. 1984. Egg production of the marine, planktonic copepod *Calanus pacificus* Brodsky: laboratory observations. *Journal of Experimental Marine Biology and Ecology*, 74: 53–66.
- Sasaki, K., Yamashita, K., and Kuroda, K. 1985. Fine distributions of nutrients in the Kuroshio Front, south of Cape Shionomisaki, Japan. *Bulletin of Tokai Regional Fisheries Research Laboratory*, 118: 1–10.
- Toda, H. 1989. Surface distributions of copepods in relation to regional upwellings around the Izu Islands in summer of 1988. *Journal of the Oceanographic Society of Japan*, 45: 251–257.
- Tsuji, S. 1985. The ecology of Japanese anchovy larvae in the Shirasu fishery. *Aquabiology*, 7: 353–358.
- Watanabe, T. 1982. Distribution of eggs and larvae of neritic migratory fish in relation to the Kuroshio. *Bulletin of Coastal Oceanography*, 19: 149–162.
- Yoder, J., Atkinson, L., Lee, T., Kim, H., and McLain, C. 1981. Role of Gulf Stream frontal eddies in forming phytoplankton patches on the outer southeast shelf. *Limnology and Oceanography*, 26: 1103–1110.

Studies on the lower trophic levels in the sea area off east coast of Honshu in spring of 1994

Y. Endo, T. Oshima, K. Sato, T. Akiho, R. Iino, H. Katsurada, N. Kuwabara, and T. Miura
(Faculty of Agriculture, Tohoku University)

Lower trophic levels in the sea area off east coast of Honshu were investigated in spring of 1994. Oceanographic observations were made with CTD systems at 45 stations. Water samples were collected with Niskin bottles attached to the CTD systems from the surface to 1000 m depth at 2 stations and to 200 m depth at 28 stations (Fig. 1). Chlorophyll *a* and nutrients were analyzed on those water samples. The twin Norpac net (110 μm and 330 μm mesh aperture) was hauled from 150 m depth to the surface to collect micro-phytoplankton and zooplankton at 30 stations. MTD nets were towed simultaneously at 12 different depth layers from the surface to 800 m at 3 stations. Chlorophyll *a* concentrations were determined by fluorometric method for total chlorophyll and chlorophyll $>10 \mu\text{m}$. Nutrient concentrations were determined with a BRAN+RUEBBE Autoanalyzer (TRAACS 800) of Tohoku National Fisheries Research Institute.

By examining T-S diagrams and NOAA images on surface water temperature, stations were judged to belong to the following water types:

- Stns. K95 and 96; Kuroshio Extension
- Stns. K75, 76, 83 and 107; Oyashio area
- Stns. K87-92; warm-core ring 93A
- Stns. K77-82, 85; another warm-core ring
- Stns. K120; the Warm Water Tongue
- Other stations; Mixed water area

Stns. K75 and 76 were located at the southern tip of the First Oyashio branch. Stns. K83 and K107 were thought to be isolated cold water areas.

Nutrients ($\text{NO}_3\text{-N}$, $\text{PO}_4\text{-P}$ and Si) increased from the surface to 200 m depth at Stn. K83 in the Oyashio area. Total chlorophyll *a* concentration had a maximum of $1.5 \mu\text{g l}^{-1}$ at 15 m depth and decreased at deeper depths, less than $0.1 \mu\text{g l}^{-1}$ from 75 m to 200 m depth. Chlorophyll $>10 \mu\text{m}$ was very low, less than $0.1 \mu\text{g l}^{-1}$ throughout the sampling depths. Similar vertical distribution of chlorophyll *a* was found at Stn. K107, an isolated cold water area. Water samples were not collected at 2 stations located at the southern tip of the First Oyashio branch.

In warm-core ring 93A nutrients gradually increased from the surface to the depths as in the Oyashio area. The maximum chlorophyll *a* concentrations were found at 10-20 m depth with $0.9 \mu\text{g l}^{-1}$ or less. Chlorophyll *a* > $10 \mu\text{m}$ was as high as about half that of total chlorophyll *a*. In another warm-core ring nutrients increased from 40 m to 75 m depth to some extent but were stable at deeper depth until 300 m depth with $\text{NO}_3\text{-N}$ concentration of about $8 \mu\text{g-at. l}^{-1}$. Maximum chlorophyll *a* concentration was $0.88 \mu\text{g l}^{-1}$ at 10 m depth.

At the Warm Water Tongue nutrient concentrations had a peak at 100 m depth with $\text{NO}_3\text{-N}$ concentration of $23 \mu\text{g-at. l}^{-1}$. Chlorophyll *a* concentration was very high, reaching $4.7 \mu\text{g l}^{-1}$ at 10 m depth. Chlorophyll *a* > $10 \mu\text{m}$ was about half that of total Chlorophyll *a* concentration.

In this study, micro-phytoplankton includes diatoms, silicoflagellates and dinoflagellates which were collected with Norpac net with $110 \mu\text{m}$ mesh aperture. Microzooplankton includes tintinnids, foraminiferans, radiolarians, and copepod nauplii which were also collected with Norpac net with $110 \mu\text{m}$ mesh aperture. Although microzooplankton were also collected with $330 \mu\text{m}$ mesh net, their abundance was generally 3-4 orders of magnitude, 1-2 orders of magnitude, and 2 orders of magnitude lower than that collected with finer mesh net. Therefore, macrozooplankton in this study includes total plankton collected with $330 \mu\text{m}$ mesh net minus microzooplankton.

Cell number of total phytoplankton was least, $0.4 \times 10^3 \text{ cells m}^{-3}$, at Stn. K75 and maximum, $2.2 \times 10^7 \text{ cells m}^{-3}$, at Stn. K115 (Fig. 2). Stns. K105, K106 and K107 were unique in that the phytoplankton cell number was fairly smaller than the other stations, and the percentage of dinoflagellates was high. Dinoflagellates represented 48 % of total phytoplankton cell number at Stn. K107.

In cell number, cold neritic species dominated total diatom assemblage especially at northern stations (Stns. K75-77, 79, 81, 82, 85 and 86), occupying more than 59 %, and at Stns. K89, 90, 92-94, 105-107, 116 and 120, occupying 31-55 %. These cold neritic diatoms consisted mainly of *Coscinodiscus wailesii* and *Chaetoceros decipiens* in northern stations and of *Chaetoceros debile* and *Ch. decipiens* in the other stations. The percentage of cold oceanic species decreased from April (KT-94-4 cruise of Tansei Maru) to June, but was still high at Stn. K83, 84 and 107, occupying 27 %, 21 % and 12 %, respectively of total diatom cell number. The percentage of warm water diatom species increased from April to June in the central-southern survey area, especially so at the Kuroshio Extension (Stn. K96) attaining 57 %. In the coastal area (Stns. K114-116, and 120), neritic species predominated, occupying more than 85 % of warm-water diatom species.

Among dinoflagellates, neritic-oceanic cold water species, *Ceratium tripos*, dominated, occupying up to 98 % of total dinoflagellates at the northern stations (Stns. K76-87 and K105-107). Warm neritic species such as *Ceratium fusus* dominated at the southern stations.

The indicator species of Kuroshio increased both in species number and cell number from April to June in the southern survey area, indicating strong effect of the Kuroshio Current in June.

Distribution of microzooplankton was similar to that of micro-phytoplankton (Fig. 3). At those stations where microzooplankton were abundant, tintinnids were dominant. Copepods dominated microzooplankton at 21 out of 30 stations, with maximum abundance of 11,640 indiv. m^{-3} at Stn. K94.

Total macrozooplankton were distributed more or less evenly in the survey area (Fig. 4). The minimum abundance was observed at Stn. K75 (100 indiv. m^{-3}) and the maximum at Stn. K77 (1,443 indiv. m^{-3}). Copepods represented 18.9-93.3 % of total macrozooplankton with the mean value of 63 %. Copepod contribution was least at Stn. K108 where copepod abundance was only 70 indiv. m^{-3} and euphausiid eggs were abundant (215 indiv. m^{-3}). A warm-water copepod genus, *Corycaeus* were abundant at Stns. K77-82, 88 and 106, with maximum numerical density of 208 indiv. m^{-3} at Stn. K106. A cold-water copepod, *Eucalanus bungii bungii* was abundant at northern stations (Stns. K76, 77, 80, 83 and 84) with the maximum density of 95 indiv. m^{-3} at Stn. K84. Doliolids were abundant in warm-core ring 93A and at Stns. K105 and 114 with the maximum abundance of 236 indiv. m^{-3} at Stn. K89.

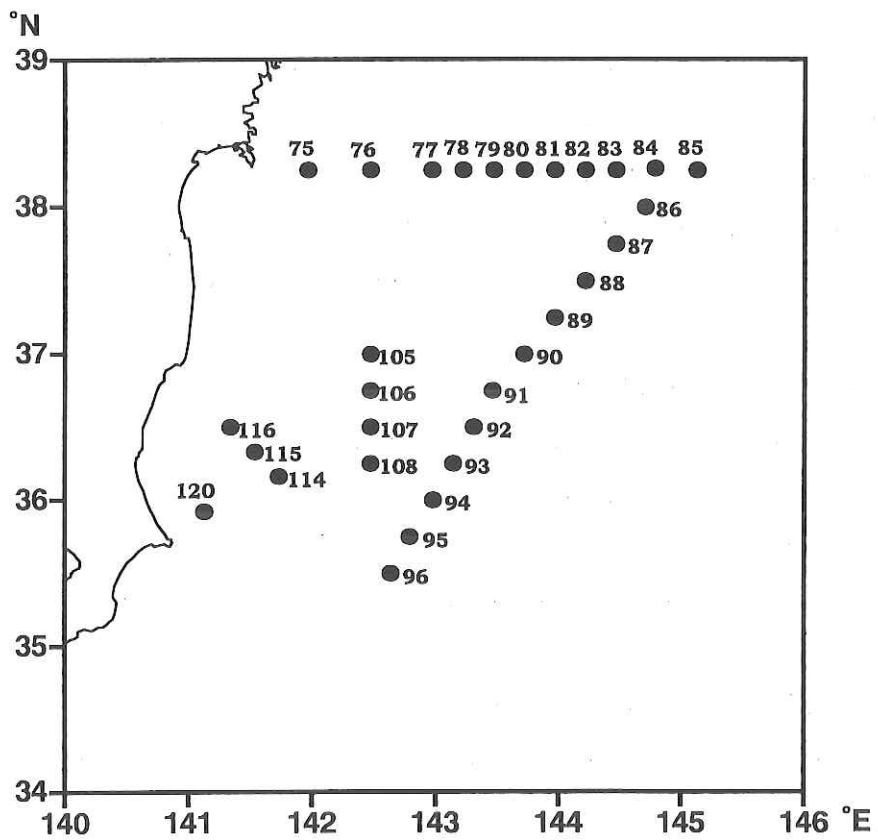


Fig. 1. Locations of sampling stations during KH-94-2 cruise of Hakuho Maru.

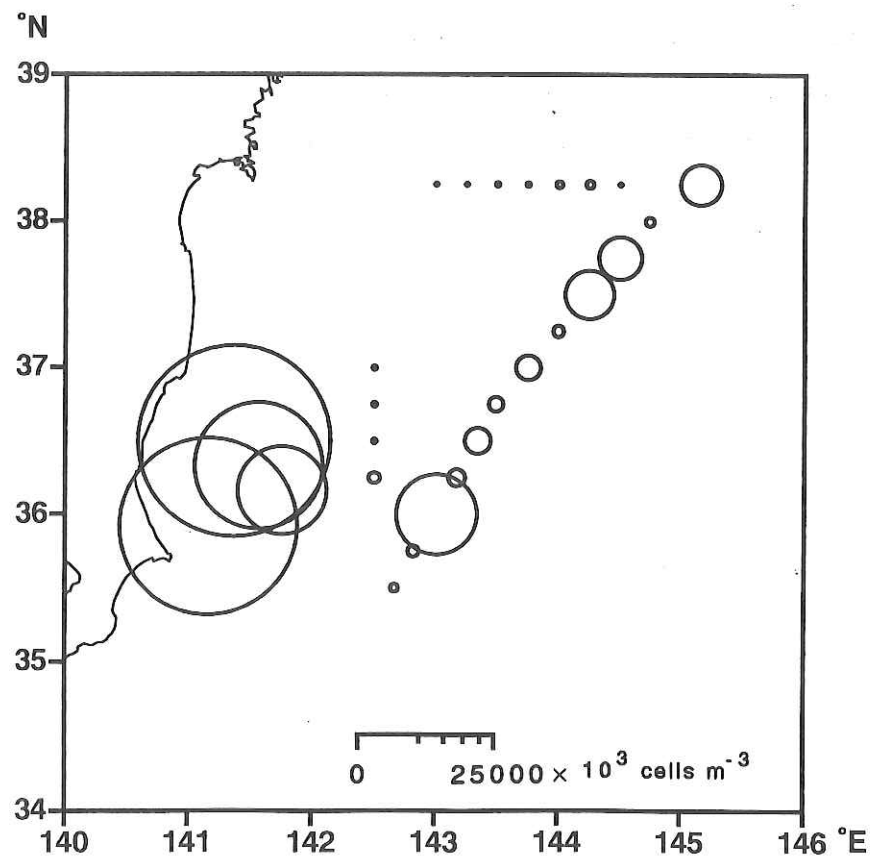


Fig. 2. Distribution in abundance of micro-phytoplankton cell number ($\times 10^3$ cells m^{-3}) which were collected with $110\ \mu m$ mesh of the twin Norpac net.

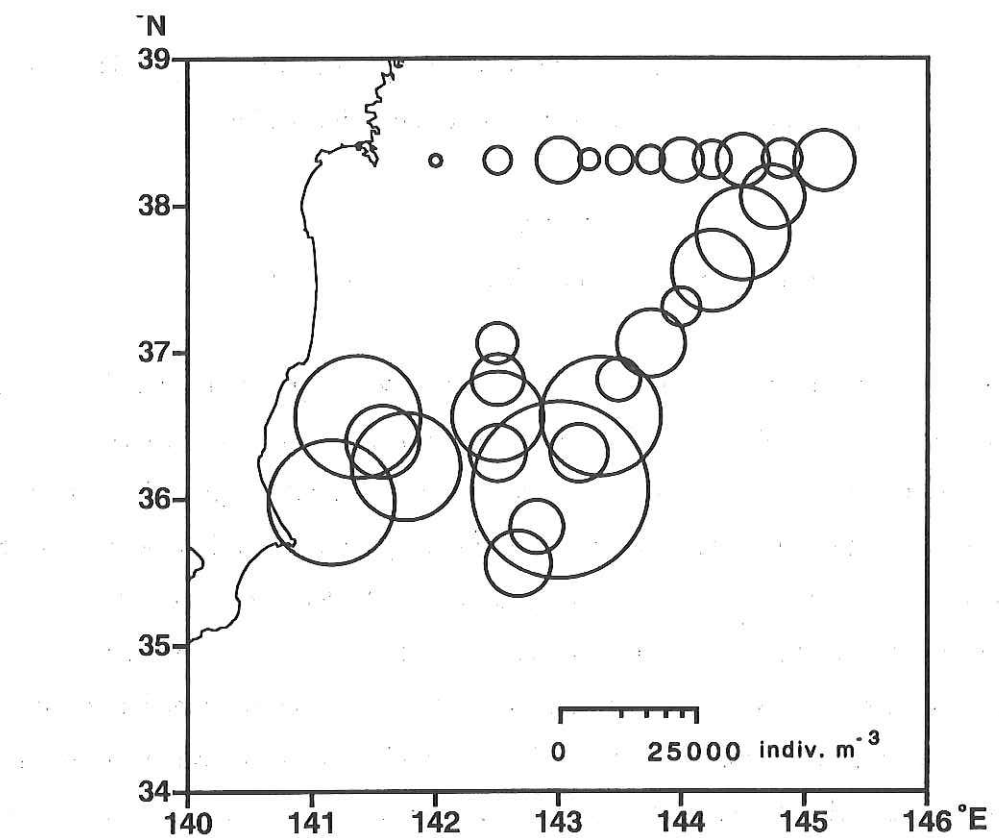


Fig. 3. Distribution in abundance of microzooplankton (indiv. m^{-3}) which were collected with 110 μm mesh of the twin Norpac net.

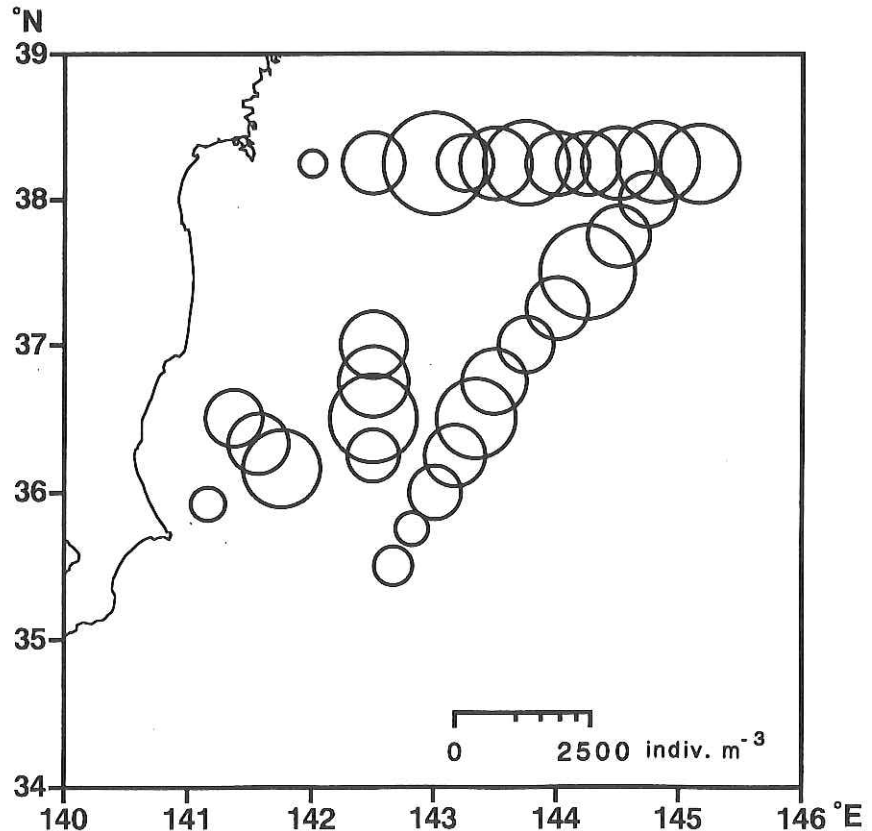


Fig. 4. Distribution in abundance of macrozooplankton (indiv. m^{-3}) which were collected with 330 μm mesh of the twin Norpac net.

Preliminary experiment for the application of the FDC (frequency of dividing cells) technique
to determine *in situ* growth rates of oligotrichous ciliates

T. Ota

(Faculty of Agriculture, Tohoku University)

Onboard culture experiments were conducted to determine the diel pattern of cell division and to measure the time duration of one cell division (Td). Surface water was collected by the acid-cleaned bucket at stations K-83 and K-108. The water was filtered through a 330 mm mesh net into 20-l plastic bag, which was incubated in a constant temperature aquarium at ambient sea surface temperatures under the 8000 lux light intensity on a 14:10 light: dark cycle. A 500 ml of sample was taken from the bag at 2 hr intervals over 24 hr, then organisms were preserved with a modified Bouin's fixative at final concentration of 5 %. On return to the laboratory, samples were stained using a Protargol method for observation of the nuclear events during asexual reproductive cycle of ciliates. Individual ciliates were examined under a microscopy at 400 x or 1000 x magnification. The analyses are now underway.

Maturation and spawning of Japanese chub mackerel *Scomber japonicus* and sardine *Sardinops melanostictus*

Ichiro Aoki¹, Tomohide Yamada¹, and Teruhisa Komatsu²

¹Department of Aquatic Bioscience, University of Tokyo

²Ocean Research Institute, University of Tokyo

Introduction

Spawning pattern is a fundamental element in understanding fish-stock variability in the context of life-history strategies in which individuals reproduce. The area around Izu Islands is one of the main spawning grounds of small pelagic fishes such as chub mackerel and sardine.

This study investigated distribution and spawning pattern of sardine and mackerel in relation to water temperature, chlorophyl and zooplankton distributions in the spawning grounds.

Methods

The surveys consisted of grid surveys with wide areal coverage around Izu Islands. Acoustic observations were made with 50kHz echo sounder, a Furuno FQ71, mounted on the RV 'Hakuho Maru' to quantify fish and zooplankton. The acoustic system processed echoes and output the mean volume backscattering strength (SV in dB) in real time for nine 10 m depth strata from 10 to 100m at horizontal integration intervals of 0.5 nautical miles (nm). Each 0.5 nm × 10 m segment was classified by observing echograms: one (fish echo) where echotraces of pelagic schooling fish occurred, and the other (plankton echo) where only weak diffuse scattering layers due to plankton appeared.

Surface temperature, salinity and chl-a concentration were measured along tracklines throughout the surveys. CTD and XBT casts were also made to determine oceanographic structure in the survey area. Sardine and mackerel were sampled with gill nets and fishing lines. The scaled body length and body weight of collected fish were measured and used for calculations of target strength and biomass. Maturity data were also obtained from the samples.

For chub mackerel, plasma levels of sex steroid hormones were measured. As soon as the fish were released from the net or angles, blood was collected from some females. Blood samples were taken from the caudal vasculature with a syringe and needle. After centrifugation, the plasma samples were frozen and kept at -20°C. The plasma levels of estradiol - 17 β (E₂) and 17 α , 20 β - dihydroxy 4 - pregnen - 3 - on (diOH) were measured according to Kagawa et al. (1981, 1982) and Young et al. (1983), respectively.

Results and Discussion

(1) Distribution of chl-a concentration

Chl-a distribution is illustrated in Fig. 1, and SST is shown in Fig. 2. At the time of the survey, the Kuroshio flowed northeastward north of Miyake-jima Island. The chl-a concentration was $0.5\text{-}1 \mu\text{g/l}$ as a whole in the coastal side of the Kuroshio, and very low in the Kuroshio waters. A high concentration area occurred off Suruga Bay.

(2) Distribution of zooplankton abundance

Fig. 2 shows SST and 5 nm mean SV excluding fish echoes for 10-50 m depth which indicates zooplankton abundance. The zooplankton biomass were distributed in accordance with the SST and Kuroshio current: it was high in the waters between 21°C and 23°C corresponding to the Kuroshio front and low in the coastal region. The zooplankton abundance increased with water temperature, and showed an inverse distribution pattern against that of chl-a concentration.

(3) Distribution of pelagic fish schools

Fish schools occurred in the coastal waters, and fish sampling indicated that they were sardine, chub mackerel and jack mackerel. Fish schools that occurred in the depth < 50 m were sardine (Fig. 3) and those in the depth > 50 m were chub mackerel and/or jack mackerel (Fig. 4).

Fig. 5 shows 5 nm mean SV from fish echoes in the 10-50 m depth. Fish schools were concentrated in the coastal side of the line drawn between Omurodashi and Zenisu shoals where $\text{SST} < 21^\circ\text{C}$. The concentration area corresponded with the area of high chl-a abundance, but did not with zooplankton abundance. Mean area backscattering strengths of the survey area were -60.5 dB for the 10-50m depth and -65.2 dB for the 50 - 100 m depth. Given that all fish echoes in the 10-50m depth were due to sardine, fish abundance was calculated to be 27,000 ton.

(4) Spawning of chub mackerel and sardine

For histological observations of ovaries, paraffin sections of ovary portions were prepared, stained by HE, and checked for the presence of postovulatory follicles.

Sardine

GSI (Gonad Somatic Index = gonad weight / body weight $\times 100$) of females and males were very low in May compared with those in March and April (Fig. 6). Ovarian histological examinations showed that sardine females were at the yolk vesicle stage and that no postovulatory follicle was found in the ovaries. Sardine had terminated spawning in this area in May. In contrast, condition factor (CF = body weight without gonad / cube of body length $\times 1000$) increased in May (Fig. 7), which showed that sardine entered the feeding period after spawning season.

Chub mackerel

Sex steroid hormones, E_2 and diOH were measured for 33 females and 34 females, respectively. Plasma E_2 was lowest at the perinucleolar stage, increased along with the yolk accumulation, and reached the highest value at the tertiary yolk globule stage, but decreased afterwards (Fig. 8). One female that had hydrated oocytes (HO) was at a low level of E_2 , and its oocytes except hydrated ones were at the primary yolk globule stage. Another female in the act of spawning (HO+PO^a) showed a relatively high E_2 concentration (5 ng/ml). This female had the tertiary yolk globule oocytes. Females that had postovulatory follicles within 1 day (PO^a) and 2 days (PO^b) after ovulation were at the tertiary yolk globule stage. These females exhibited high levels of E_2 comparable to females at the secondary and tertiary yolk globule stages. On the other hand, diOH

remained at low levels at all maturity stages (Fig. 8).

Plasma levels of E₂ and diOH in chub mackerel were measured for the first time in the present study. Changes in E₂ levels of chub mackerel are in agreement with the notion that E₂ promotes vitellogenin synthesis as reported in many other fishes (e.g. Wingfield and Grimm, 1977; Fostier et al., 1983; Whitehead et al., 1983). Our results also indicate that the oocytes that had completed yolk accumulation did not produce E₂. High E₂ levels in the females with postovulatory follicles show that yolk accumulation starts again immediately after spawning. This E₂ profile may reflect short intervals in spawning of chub mackerel.

It has been reported in many fish species that diOH is secreted during final maturation and ovulation (e.g. Stacey et al. 1983; Kagawa et al. 1984; Kobayashi et al. 1987). In wild Japanese sardine, high levels of diOH were observed during final maturation (Murayama et al. 1994). However, peak of diOH concentration was not observed in chub mackerel in this study. Our female samples were captured between 1900 and 2400 hours. Measure of diOH level is likely to vary depending on diurnal maturation cycle and sampling time. It is necessary to do a lot more sampling over a longer period of time of day. Alternatively, maturation-inducing steroid (MIS) in chub mackerel may be differed from diOH. There is no study on MIS in chub mackerel. Some other steroids such as 17 α -hydroxy-5 β -pregnen-3,20-dione (Hirose et al. unpublished) function as MIS in other species. It is necessary to measure the plasma level of some kinds of steroids in order to clarify their roles during ovarian maturation.

References

- Fostier, A., Well, C., Billard, R., Breton, B., and Zohar, Y. (1983) The gonadal steroids. In Fish Physiology, Vol. 9 (A) (Hoar, W.S. et al. Eds.), pp. 277-372, New York, Academic Press.
- Kagawa, H., Takano, K., and Nagahama, Y. (1981) Cell Tissue Res. 218, 315-329.
- Kagawa, H., Young, G., Adachi, S., and Nagahama, Y. (1982) Gen. Comp. Endocrinol. 47, 440-448.
- Kagawa, H., Young, G., and Nagahama, Y. (1984) Gen. Comp. Endocrinol. 54, 139-143.
- Kobayashi, M., Aida, K., and Hanyu, I. (1987) Gen. Comp. Endocrinol. 67, 24-32.
- Murayama, T., Shiraishi, M., and Aoki, I. (1994) J. Fish Biol. 45, 235-245.
- Stacey, N.E., Peter, R.E., Cook, A.F., Truscott, B., Walsh, J.M., and Idler, D.R. (1983) Can. J. Zool. 61, 2646-2652.
- Young, G., Crim, L.W., Kagawa, H., Kambegawa, A., and Nagahama, Y. (1983) Gen. Comp. Endocrinol. 51, 96-105.
- Wingfield, J.C. and Grimm, A.S. (1977) Gen. Comp. Endocrinol. 31, 1-11.
- Whitehead, C., Bromage, N.R., and Breton, B. (1983) Aquaculture, 34, 317-326.

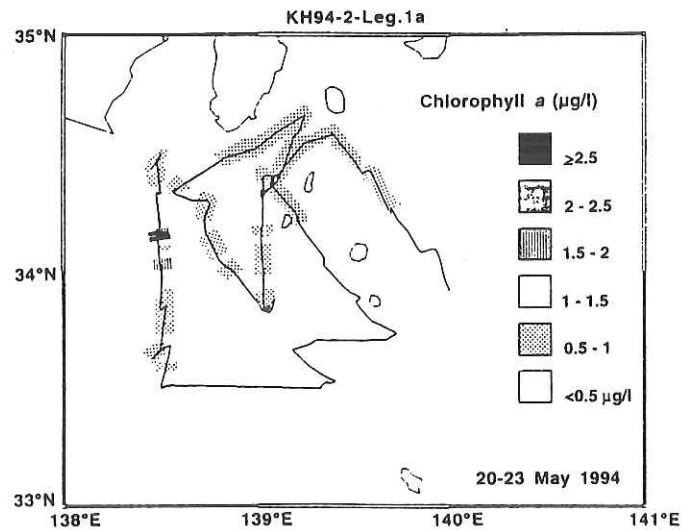


Fig. 1. Distribution of chlorophyl-a

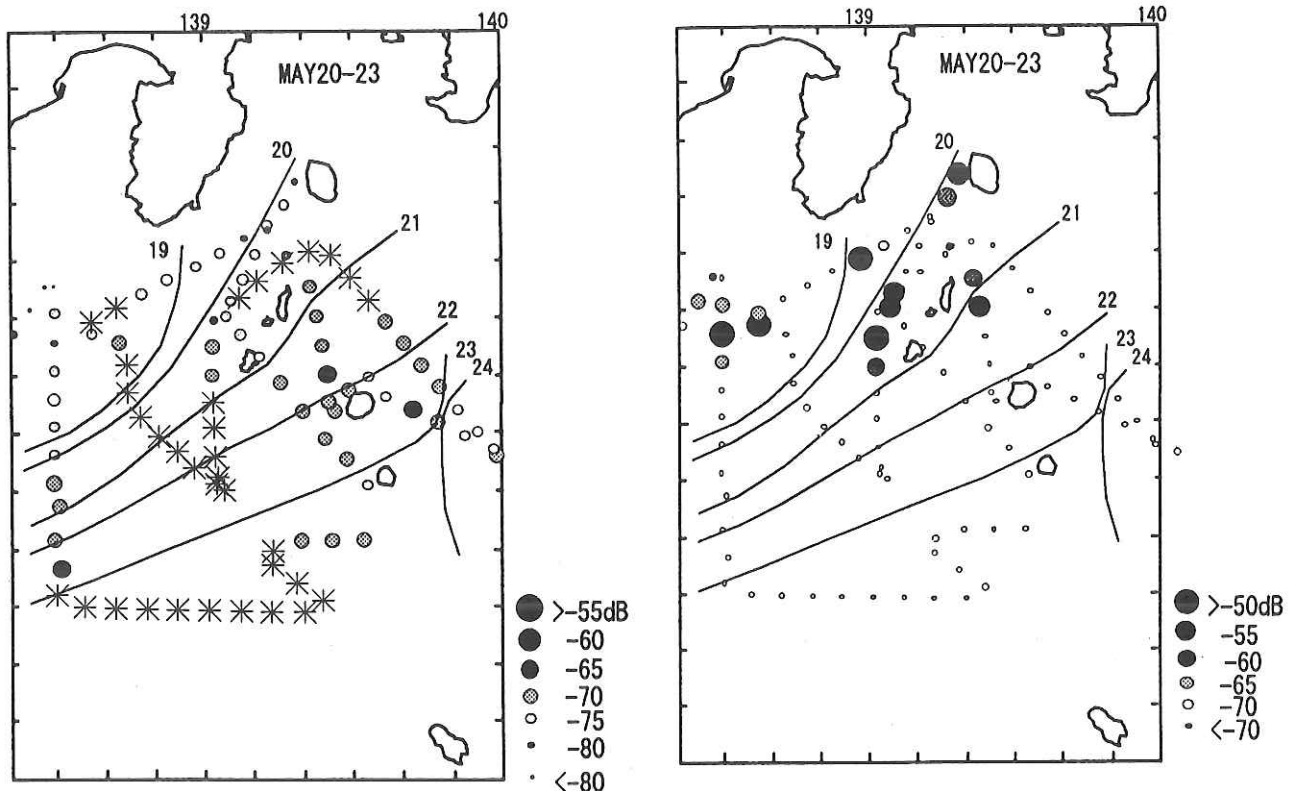


Fig. 2. Distribution of SV from zooplankton (10-50m depth, 5nm segment). SV values in daytime segments are shown and asterisks indicate nighttime segments excluded in analysis.

Fig. 5. Distribution of area backscattering strength (SA) from fish schools (10-50 m depth, 5nm segment).

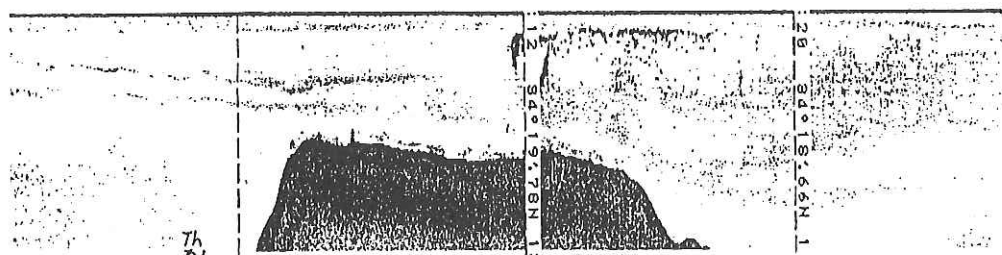


Fig. 3. Ecotrace of sardine schools at 50 kHz in the 200 m depth range. At Hyotan-se, west of Nii-jima, May 21, 1994.



Fig. 4. Ecotrace of chub mackerel and/or jack mackerel schools at 50 kHz in the 200 m depth range. At Hyotan-se, west of Nii-jima, June 8, 1994.

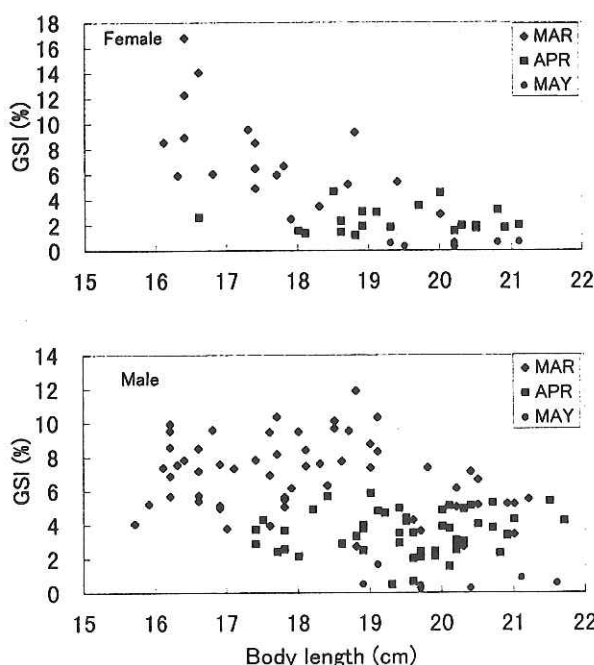


Fig. 6. GSI in individuals plotted against body length in March (KH-94-1), April (KT-94-5) and May (this cruise).

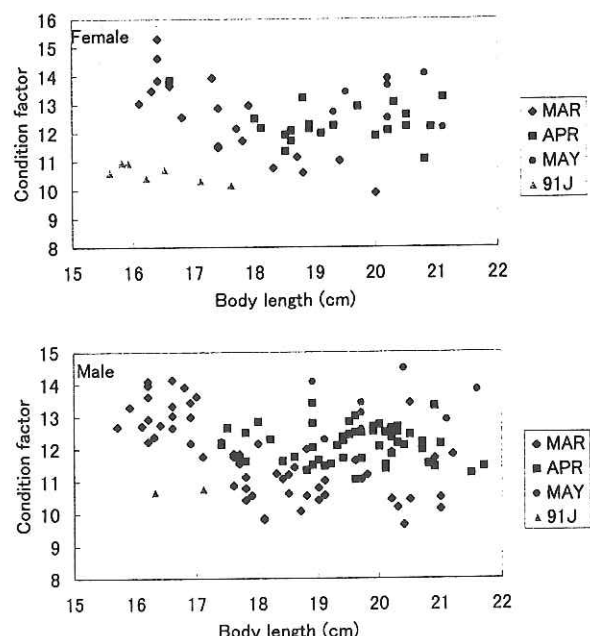


Fig. 7. Condition factor in individuals plotted against body length in March (KH-94-1), April (KT-94-5) and May (this cruise).

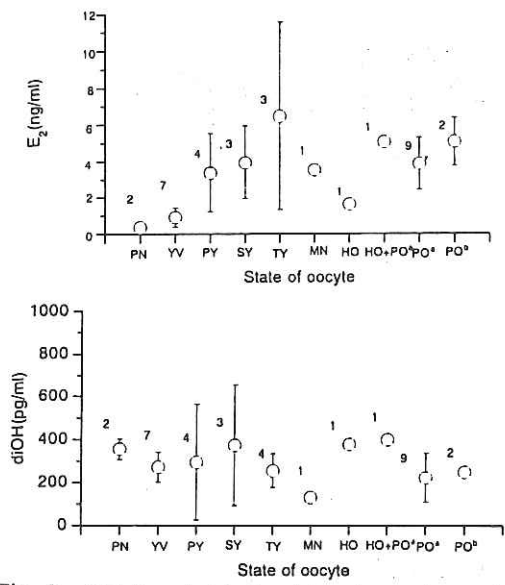


Fig. 8. Relation between state of oocyte, postovulatory follicles and change of the levels of E_2 (estradiol-17 β) and diOH ($17\alpha, 20\beta$ -dihydroxy-4-pregnen-3-one).

PN: perinucleolar stage
 YV: yolk vesicle stage
 PY: primary yolk globule stage
 SY: secondary yolk globule stage
 TY: tertiary yolk globule stage
 MN: migratory nucleus stage
 HO: hydrated oocytes
 HO+PO*: hydrated oocytes and postovulatory follicles within 1day after ovulation
 PO*: postovulatory follicles within 1day after ovulation
 PO*: postovulatory follicles 1 day to 2day after ovulation

